

**Internal and Interface
Shear Strength of
Geosynthetic Clay Liners (GCLs):
Additional Data**

by

John McCartney
Jorge Zornberg
Robert H. Swan, Jr.

A report submitted to the
Department of Civil, Environmental and Architectural Engineering
University of Colorado at Boulder
June 2002

McCartney, John S., Zornberg, Jorge G., and Swan, Jr., Robert H.

Internal and Interface Shear Strength of Geosynthetic Clay Liners (GCLs): Additional Data

Geosynthetic Clay Liners (GCLs) are prefabricated geocomposite materials used as an alternative to compacted clay liners in hydraulic barriers. They often offer hydraulic performance equivalent to that of compacted clay liners with lower costs, easier constructability and less space requirements. However, the internal and interface shear strength of GCLs is known to be significantly lower than that of compacted clay liners, so their use in a landfill cap or base liner system requires a careful shear strength assessment. Because of the significant time and effort involved in GCL shear strength testing, clear understanding of shear strength data collected for this material may provide insight that complements often limited project-specific testing conducted for engineering design.

The internal and interface shear strength of GCLs were investigated by the previous report by McCartney, Zornberg and Swan, Jr. (2002). This report contains additional data to reinforce the understanding of the variability in internal and interface shear strength of needle-punched and unreinforced GCLs. In addition, data is presented to link the variability in the shear strength to the peel-strength of the GCLs.

1 Introduction.....	5
2 Update of Equivalent Friction Angle Analysis with Additional Data.....	5
3 Discussion of Variability of Internal and Interface Shear Strength of Unreinforced GCLs.....	5
4 Discussion of Variability of Internal and Interface Shear Strength of Reinforced GCLs	6
4.1 GCL-Geomembrane Interface Shear Strength.....	7
4.2 Internal GCL Shear Strength	8
4.3 Correlation and Shear Strength Parameter Probability Distributions	8
4.4 Effect of Peel Strength	9
5.0 Conclusions.....	11
Additional References.....	36

Table 1: Updated Equivalent Friction Angles for the Shear Strength of the Interface between a GCL and a Geomembrane	12
Table 2: Updated Equivalent Friction Angles for Internal GCL Shear Strength.....	13
Table 3: Failure Envelopes for GCL F	14
Table 4: Variability Analysis for GCL F with Comparison to GCL A Tested Under Similar Conditions.....	14
Table 5: Failure Envelopes for the Interface between GCL K and a THDPE Geomembrane	14
Table 6: Shear Strength of the Interface between GCL A and an 80-mil Textured HDPE Geomembrane s ($t_H = 168$ hours, $t_C = 48$ hours, SDR = 0.1 mm/min).....	15
Table 7: Internal Shear Strength of GCL A ($t_H = 168$ hours, $t_C = 48$ hours, SDR = 0.1 mm/min)	16
Table 8: Statistical Analysis of the Shear Strength of the Interface between GCL A and an 80-mil Textured HDPE Geomembrane s Interface ($t_H = 168$ hours, $t_C = 48$ hours, SDR = 0.1 mm/min).....	17
Table 9: Statistical Analysis of the Internal Shear Strength of GCL A ($t_H = 168$ hours, $t_C = 48$ hours, SDR = 0.1 mm/min).....	17
Table 10: Summary of the Failure Envelope Data for the Shear Strength of the Interface between GCL A and an 80-mil Textured HDPE Geomembrane s and the Internal Shear Strength of GCL A ($t_H = 168$ hours, $t_C = 48$ hours, SDR = 0.1 mm/min)	17
Table 11: Peel Strength for GCL A; Included are the Series Number in Which the GCL was Tested for Internal or Interface Shear Strength in Tables 6 and 7	18
Figure 1: Internal Shear Strength Failure Envelopes for GCL F (a) Peak, (b) Large Displacement	19
Figure 2: Variation in Peak and Large Displacement Shear Strength of GCL F Sheared at a Normal Stress of 9.6 kPa	19
Figure 3: Probability Density Functions for the Shear Strength of GCL F: (a) Peak and (b) Large Displacement.....	20
Figure 4: Failure Envelopes for the Interface between GCL K and a Textured HDPE Geomembrane, Effect of the Time of Hydration (a) Peak, (b) Large Displacement.....	21
Figure 5: New Shear Strength Data for the Interface between GCL A and an 80-mil Textured HDPE Geomembrane s ($t_H = 168$ hours, $t_C = 48$ hours, SDR = 1.0 mm/min).....	24

Figure 6: New Shear Strength Data Combined with Existing Data for the Interface between GCL A and an 80-mil Textured HDPE Geomembrane s ($t_H = 168$ hours, $t_C = 48$ hours, SDR = 1.0 mm/min).....	25
Figure 7: New Internal Shear Strength Data for GCL A ($t_H = 168$ hours, $t_C = 48$ hours, SDR = 1.0 mm/min).....	26
Figure 8: New Internal Shear Strength Data Combined with Existing Data for GCL A ($t_H = 168$ hours, $t_C = 48$ hours, SDR = 1.0 mm/min).....	27
Figure 9: Correlation Plots for the Intercept Value and Friction Angle for the Peak and Large Displacement Shear Strength Failure Envelopes, (a) GCL A Interface with a Textured HDPE Geomembrane s, (b) Internal GCL A	28
Figure 10: Probability Density Functions for the Peak Failure Envelope for the Interface between GCL A and a Textured HDPE Geomembrane s; (a) Intercept Value, (b) Friction Angle....	29
Figure 11: Probability Density Functions for the Peak Internal Failure Envelope for GCL A; (a) Intercept Value, (b) Friction Angle.....	30
Figure 12: Modified Reliability Based Design Chart for for the Interface between GCL A and a Textured HDPE Geomembrane s; (a) Peak Shear Strength, (b) Large Displacement Shear Strength.....	31
Figure 13: Modified Reliability Based Design Chart for for the Interface between GCL A and a Textured HDPE Geomembrane s; (a) Peak Shear Strength, (b) Large Displacement Shear Strength.....	32
Figure 14: Probability Distribution for the Peel Strength of GCL A (5 Tests on 15 Specimens, Total of 75 Tests).....	33
Figure 15: Relationship between Peel Strength and Peak Internal Shear Strength of GCL A	33
Figure 16: Relationships between Peel Strength and Peak Internal Shear Strength of GCL A for Normal Stresses of: (a) 34.5 kPa, (b) 137.9 kPa and (c) 310.3 kPa.....	34
Figure 17: Relationship between Peel Strength and Peak Interface Shear Strength of GCL A ...	35

1 Introduction

All GCL and geomembrane name designations are the same as in McCartney *et. al.* (2002). Additional data has been presented for the variability of the shear strength of the interface between GCL *A* and an 80-mil GSE textured HDPE geomembrane as well as the internal shear strength of unreinforced GCL *F* and needle-punched GCL *A* specimens. The new data is presented in this report in addition to several modified figures from McCartney *et. al.* (2002).

2 Update of Equivalent Friction Angle Analysis with Additional Data

Tables 1 and 2 show the updated equivalent friction angles for interface and internal GCL shear strength, respectively. Recall that the upper and lower bounds are equal to the average plus or minus two times the standard deviation. Standard deviations were developed for the sensitivity analysis (to GCL type, geomembrane manufacturer and geomembrane thickness) for the interface GCL shear strength.

3 Discussion of Variability of Internal and Interface Shear Strength of Unreinforced GCLs

Five new direct shear tests were run on the internal shear strength of a GCL *F*, which is an unreinforced layer of sodium bentonite mixed with adhesives, bonded to a woven geotextile and a nonwoven geotextile. Although there were few tests conducted on unreinforced GCLs as part of the GCLSS database, the lower variability in shear strength of unreinforced GCLs than that for reinforced GCL implies that fewer tests will adequately describe the variability. Table 3 shows all of the failure envelopes for GCL *F*, including a new set of 5 tests conducted on GCL *F* tested at a normal stress of 9.6 kPa with a time of hydration of 24 hours, no consolidation and a shear displacement rate of 1.0 mm/min. All three failure envelopes are shown in Figures 1(a) and 1(b).

The five new tests conducted on the internal shear strength of GCL *F* provide an excellent opportunity to assess the variability of unreinforced GCLs. Table 5 shows the results of a statistical analysis on these five tests, along with statistical analyses for GCL *A* conducted under similar conditions. Figure 2 shows a histogram of the peak and large displacement shear strengths for these five tests. Although the average peak and large displacement shear strength of this GCL are relatively low, the standard deviation values are comparatively high (*i.e.* COV

values between 15 and 19%). The correlation coefficient between the peak and large displacement shear strengths is strongly positive, implying a non-linear increasing trend between the peak shear strength and the amount of post-peak shear strength reduction. Figures 3(a) and 3(b) show probability density distributions built from these five data points. It is clear that these distributions are incomplete due to the small sample size, but further tests may indicate a uniform (constant probability for obtaining shear strength values between a certain range of shear strength) or lognormal distribution.

In addition to the new variability tests for GCL *F*, a new test series for the shear strength of the interface between GCL *K* and a 30-mil textured HDPE geomembrane with a time of hydration of 24 hours, no consolidation and a shear displacement rate of 1.0 mm/min has been obtained. This new failure envelope is shown in Figure 4 and Table 5. It is interesting that the interface hydrated for 24 hours is significantly weaker than that hydrated for 48 hours. This may indicate inadequate or unpredictable hydration conditions in the GCL *K* interfaces due to sodium bentonite encapsulations between the geomembranes.

4 Discussion of Variability of Internal and Interface Shear Strength of Reinforced GCLs

A total of 22 new tests were run on the interface shear strength of GCL *A* and an 80-mil GSE textured HDPE geomembrane, as well as 15 new tests run on the internal shear strength of GCL *A*. Tables 6 and 7 show the interface and internal shear strength values for all of the 41 and 34 test series, respectively, for GCL *A* and a textured HDPE geomembrane s hydrated for 168 hours, consolidated for 48 hours and sheared at a shear displacement rate of 0.1 mm/min. This data was used to develop new failure envelopes, PDF plots, correlation analyses, and shear strength parameters.

The large number of tests in the GCLSS database allows assessment of the variability of GCL internal τ_p and τ_{ld} . Considering that GCLs are composite materials, the variability analysis presented herein allows identification of different potential sources of variability of shear strength results. In addition, quantification of the variability of internal shear strength results provides relevant information for reliability-based limit equilibrium analyses. Potential sources of variability in GCL internal shear strength include: (i) differences in GCL reinforcement and carrier geosynthetic types, (ii) differences in test equipment and procedures among different

laboratories, (iii) effect of σ_n and test conditions, (iv) inherent variability in reinforcements, (v) inherent variability in the shear strength of sodium bentonite clay.

The number of shear strength test results in the GCLSS database is large enough to provide representative samples for assessment of several sources of variability. The first source of variability listed above is avoided in this study by assessing the variability of individual GCL types. The second source of variability can be assessed by considering data obtained from a single laboratory using consistent testing procedures on specimens from a single manufactured lot. Figure 5(a) shows shear stress-displacement curves for GCL A specimens obtained from the same lot but different rolls. Although the δ_p values are slightly different, the behavior is nearly identical at each σ_n . Figure 5(b) shows the τ_p and τ_{ld} envelopes from the results of these curves. It should be noted that the coefficient of variation (COV = Standard deviation divided by the mean) value for each pair of tests are less than 0.03, which, as will be shown below, is insignificant compared to the variability that arises when observing GCLs from different lots. Figures 6(a) and 6(b) show the results of another set of tests on GCL A specimens taken from a different lot and different shear displacement rate. The same consistency is noted. The remaining potential sources of variability are evaluated by evaluating the variability of multiple GCLs tests conducted using the same σ_n and test conditions, evaluating the variability of GCL peel strength, which has been considered an index of the reinforcement contribution, and evaluating the variability in shear strength of unreinforced GCLs.

4.1 GCL-Geomembrane Interface Shear Strength

The new GCL-geomembrane interface peak and large displacement shear strength test results are shown alone in Figure 7(a) and 7(b). These figures were compiled to check that the new test data was relatively similar to the test data reported by McCartney et. al. (2002) for the same GCLs and geomembranes tested under similar conditions. All 41 tests series are shown in Figures 8(a) and 8(b), along with the probability density distributions for each normal stress. The mean and standard deviations for the shear strength at each normal stress level are shown in Table 8 (developed from the data in Table 6). The mean value for peak and large displacement conditions did not change greatly from what was reported by McCartney *et. al.* (2002), but the standard deviation values are slightly higher. The probability distributions for the shear strength

data at each normal stress level resemble lognormal distributions. This will prove important for a reliability based design.

4.2 Internal GCL Shear Strength

The new peak and large displacement internal GCL shear strength test results are shown alone in Figure 9(a) and 9(b). These figures were compiled to check that the new test data was relatively similar to the test data reported by McCartney *et. al.* (2002) for the same GCLs and geomembranes tested under similar conditions. All 34 tests series are shown in Figures 10(a) and 10(b), along with the probability density distributions for each normal stress. The mean and standard deviations for the shear strength at each normal stress level are shown in Table 9 (developed from the data in Table 7). Again, the mean value for peak and large displacement conditions did not change greatly from what was reported by McCartney *et. al.* (2002), and the standard deviation values are slightly higher. In addition, the probability distributions for the shear strength data at each normal stress level again resemble lognormal distributions.

4.3 Correlation and Shear Strength Parameter Probability Distributions

The Mohr-Coulomb shear strength parameters (c and ϕ) were calculated for each test series presented in Tables 6 and 7 for the interface and internal GCL shear strength, respectively. A statistical analysis was then conducted on these shear strength parameters, and the results are presented in Table 9. This table shows that the intercept value is much more variable than the friction angle value. In addition, it is interesting to view the correlation between the shear strength parameters. Figures 11(a) and 11(b) show the correlation between the peak intercept values and peak friction angle values for interface and internal GCL shear strength, respectively. This figure shows that there is a slight negative trend in the interface shear strength and a slight positive trend in the internal shear strength. These findings may have important effects on a reliability based design. Figure 12(a) and 12(b) show the probability distributions for the peak interface GCL shear strength parameters. These figures indicate that the intercept value follows a lognormal distribution and the friction angle follows a normal distribution. Figures 13(a) and 13(b) show the same plots for the peak internal GCL shear strength parameters. Again, the intercept value follows a lognormal distribution and the friction angle follows a normal distribution.

Figures 14(a) and 14(b) show the updated reliability based design charts for the peak interface GCL shear strength, while Figures 15(a) and 15(b) show the updated reliability based design charts for the internal GCL shear strength. Only slight changes were observed in these figures from those presented by McCartney *et. al.* (2002).

5 Effect of Peel Strength

Peel strength data has been reported to provide an index of the quality of needle-punching in a GCL (Eid and Stark 1999, Bouazza 2002). The peel strength (*ASTM D6496*) involves placing the carrier geotextiles of a 100 mm wide dry GCL specimen between clamps, and measuring the force required to separate the geotextiles. The force required to separate the carrier geotextiles has been considered as a measure of the density of needle-punched fiber reinforcements. However, it should be noted that the peel strength test mobilizes the fibers in a manner that may not be representative of limitations the conditions in which the fibers are mobilized during a direct shear test.

A total of 75 peel strength tests were conducted on GCL *A* specimens. Specifically, five tests were conducted on 15 rolls of GCL *A* used in the testing program described in section 4, the results of which are shown in Table 11. Figure 16 shows the probability density function obtained from the 75 peel strength test results. Peel strength results varied significantly (43 to 225 N/100 mm). The specified values provided by the GCL *A* manufacturer is 65 N/100 mm. The relationship between the peel strength and the internal τ_p of GCL *A* specimens taken from these 15 rolls is shown in Figure 17. Details for each normal stress are shown in Figures 18(a), 18(b) and 18(c). Consistent with results reported by Richardson (1997), this figure indicates that τ_p is relatively insensitive to τ_p . A slight increasing trend between peel strength and τ_p can be observed, particularly at higher σ_n . Since the peel strength is found to be insensitive to τ_p , the inherent variability in peel strength cannot be used to explain the variability of GCLs. In addition, the relationship between the peel strength and τ_p of the interface between GCL *A* and an 80-mil THDPE geomembrane *s* is shown in Figure 19. This figure shows the same behavior as Figure 15, which implies that the peel strength is not a good indicator of interface shear strength for needle-punched GCLs.

6 Shear Displacement Rate

An additional test was conducted on the shear strength of GCL A at low normal stress and a shear displacement rate of 0.01 mm/min. This test compliments data from McCartney *et al.* (2002) on the effect of the shear displacement rate at different normal stress levels. The discussion based on this additional figure is presented below.

The effect of SDR on τ_p and τ_{ld} has been reported by Gilbert *et al.* 1997, Fox *et al.* 1998 and Eid *et al.* 1999. Although these studies focused only on the response of tests conducted under comparatively low σ_n , an increasing trend in τ_p was reported for increasing SDR. Causes proposed to explain this trend include creep and rate-dependent fiber reinforcement pullout behavior during shearing. The GCL internal residual shear strength was reported to be essentially insensitive to SDR.

The GCLSS database allows a more comprehensive analysis of the effect of SDR on internal shear strength, as it includes tests conducted at comparatively high σ_n values, which have not been reported in previous studies. Figure 20(a) shows the results of tests on GCL A conducted under low σ_n (50 kPa) under the same test conditions ($t_h = 24$ hs, $t_c = 0$ hs), but varying SDR (0.01, 0.5 and 1.0 mm/min). Consistent with the trend reported in past studies for tests conducted under low σ_n , the results show an increasing τ_p value with increasing SDR. The results also show that residual shear strength was only reached at the end of the test for the fast SDR (1.0 mm/min), while residual conditions have not been apparently reached for tests conducted at lower SDR. Figure 20(b) shows the results of tests on GCL A conducted under comparatively high σ_n (520 kPa) and the same test conditions ($t_h = 312$ hs and $t_c = 48$ hs), but varying SDR (0.0015, 0.01, 0.1 and 1.0 mm/min). Unlike the trend shown in Figure 20(a) for tests conducted under low σ_n , the results in Figure 20(b) show a decreasing τ_p with increasing SDR. However, as observed in Figure 20(a), the GCL tested at the fastest SDR (1.0 mm/min) reached residual shear strength while the other GCLs have not reached this condition at the end of the test.

Figure 20(c) summarizes the shear strength results from the tests shown in Figures 20(a) and 20(b), in addition to duplicate tests conducted to verify the repeatability of test results. τ_p decreases at a rate of approximately 15 kPa per log cycle of SDR for tests conducted at $\sigma_n = 520$ kPa, while it increases at a rate of approximately 12 kPa per log cycle of SDR for tests conducted at $\sigma_n = 50$ kPa

Although creep and rate-dependent pullout of the fiber reinforcements have been proposed in the literature to explain the effect of SDR on τ_p (e.g. Eid and Stark 1997, Gilbert *et al.* 1997 for tests conducted under comparatively low σ_n), the availability in this study of test results obtained under high σ_n suggests that the reason for the observed trends is the generation of shear-induced pore water pressures. In the case of tests conducted under low σ_n (*i.e.* below the swell pressure of GCLs), shear-induced pore water pressures are expected to be negative. Consequently, increasing SDR will lead to higher (negative) pore water pressures and thus higher τ_p values. On the other hand, tests conducted under high σ_n (*i.e.* above the swell pressure of GCLs) shear-induced pore water pressures are expected to be positive. Increasing SDR will lead to higher (positive) pore water pressures and thus lower τ_p values.

Since no shear-induced pore water pressures are expected (positive or negative), under residual (constant volume) conditions, the same residual shear strength is expected to be achieved at sufficiently large δ . Even though residual shear strength was not achieved for tests conducted using slow SDR, the tests conducted using a faster SDR reached residual shear strength conditions for comparatively small δ . Indeed, Gilbert *et al.* (1997) and Eid and Stark (1999) have reported residual shear strength results that were insensitive to the SDR irrespective of the SDR value. An important consequence of this response is that, if design is governed by residual shear strength, direct shear tests conducted using high SDR should provide adequate internal shear strength characterization.

7 Conclusions

The new data presented in this report leads to the following conclusions concerning the variability of internal and interface GCL shear strength:

- The COV of unreinforced GCLs is similar to that of reinforced GCLs (COV of approximately 0.2), suggesting that the main source of GCL variability is the inherent variability of sodium bentonite.
- Variable hydration conditions exist in the interface between GCL K and a geomembrane due to sodium bentonite encapsulation between the two geomembranes.
- Tests on a single lot were observed to be repeatable with a COV for the tests at different normal stresses less than 0.05, which is lower than the COV observed for tests conducted on GCLs taken from different rolls.

- The additional data for internal and interface GCL shear strength at constant test conditions shows that the variability data presented by McCartney *et. al.* (2002) was representative of a larger sample size.
- For linear failure envelopes developed for internal and interface GCL A shear strength:
 - The intercept value was typically more variable than the friction angle
 - The intercept value for a follows a lognormal distribution, while the friction angle follows a normal distribution.
 - The intercept value was two to three times more variable than the friction angle of the failure envelope for internal or interface GCL shear strength
- The variability in shear strength, quantified by the COV, is not particularly sensitive to σ_n or to sample conditioning.
- Peel strength was observed to have a comparatively high variability. However, the correlation between peel strength and τ_p for needle-punched GCLs was found not to be strong. Consequently, conclusions regarding the effect of the variability in fiber reinforcement density on the variability of τ_p cannot be made.
- Peak shear strength of reinforced GCLs increases with increasing SDR for low σ_n . On the other hand, the peak shear strength of reinforced GCLs decreases with increasing SDR for high σ_n . This behavior is consistent with the generation of negative pore water pressures under low σ_n (below the swell pressure) and of positive pore water pressures under high σ_n . Consequently, if design is governed by τ_p , testing using sufficiently low SDR should be specified.
- Residual conditions were achieved at a lower δ for tests conducted at a high SDR. Consequently if design is governed by τ_{ld} , testing using sufficiently high SDR should be specified.

Table 1: Updated Equivalent Friction Angles for the Shear Strength of the Interface between a GCL and a Geomembrane

Interface Set	Set Description	Peak				Large Displacement					
		Equivalent Friction Angle (Degrees)	Standard Deviation Equivalent Friction Angle (Degrees)	Upper Bound Equivalent Friction Angle (Degrees)	Lower Bound Equivalent Friction Angle (Degrees)	Equivalent Friction Angle (Degrees)	Standard Deviation Equivalent Friction Angle (Degrees)	Upper Bound Equivalent Friction Angle (Degrees)	Lower Bound Equivalent Friction Angle (Degrees)		
1	Textured Geomembrane Interfaces	21.0	2.6	26.3	15.8	12.8	2.9	18.6	7.1		
2	Smooth Geomembrane Interfaces	10.0	2.2	14.4	5.5	9.4	2.2	13.8	4.9		
3	PVC Geomembrane Interfaces	18.9	2.0	22.9	14.9	18.9	2.0	22.9	14.9		
4	TVLDPE Geomembrane Interfaces	31.7	6.5	44.7	18.7	25.1	6.3	37.7	12.5		
5	TLLDPE Geomembrane Interfaces	29.8	2.1	34.0	25.6	22.6	1.5	25.7	19.5		
6	All THDPE Geomembrane Interfaces	21.0	1.7	24.4	17.6	12.8	1.9	16.6	9.1		
7	THDPE Geomembrane Interfaces	GCL	A	21.5	1.0	23.4	19.5	12.7	1.2	14.8	10.1
8			B	13.2	5.0	23.1	3.2	9.9	4.5	18.8	1.0
9			C	21.4	1.2	22.2	17.5	12.4	1.0	15.4	11.4
10			K	25.8	0.7	27.6	25.0	16.6	1.0	18.1	14.2
11			s	20.9	1.1	22.9	18.6	13.2	1.2	15.3	10.6
12		THDPE Geomembrane Manufacturer	t	16.8	4.3	25.5	8.1	10.6	4.3	19.2	2.1
13			u	26.1	0.8	27.6	24.6	16.7	1.3	19.2	14.2
14			v	21.3	0.5	22.3	20.2	11.9	0.8	13.6	10.2
15			w	20.8	0.6	21.9	19.6	10.4	0.5	11.4	9.5
16			Geomembrane Thickness	40mil	23.0	2.9	28.9	17.2	11.3	3.0	17.4
17		60mil		20.4	2.4	25.2	15.7	12.3	2.7	17.7	6.9
18		80mil		21.6	0.9	23.3	19.8	13.6	0.9	15.2	11.6

Note: Equivalent friction angle defined for the normal stress range 0-700 kPa for each interface set

Table 2: Updated Equivalent Friction Angles for Internal GCL Shear Strength

GCL Set Number	GCL set description	Number of results in each set	Peak			Large Displacement			
			ϕ_{EQ} (Degrees)	$\phi_{EQ,u}$ (Degrees)	$\phi_{EQ,l}$ (Degrees)	ϕ_{EQ} (Degrees)	$\phi_{EQ,u}$ (Degrees)	$\phi_{EQ,l}$ (Degrees)	
1	All GCLs	354	28.0	47.6	8.4	221	10.7	14.2	7.2
2	All reinforced GCLs	331	28.6	48.6	8.7	208	10.9	14.3	7.6
3	Unreinforced GCLs	13	6.6	14.6	0.0	13	5.9	11.5	0.3
4	All needle-punched GCLs	251	30.9	49.8	12.1	161	11.1	14.5	7.8
5	Stitch-bonded GCLs	44	12.5	46.1	0.0	4	6.3	7.2	5.5
6	All thermal-bonded GCLs	46	27.9	40.0	15.8	43	11.4	16.1	6.8
7	Needle-punched W-NW	234	30.6	49.2	11.9	156	11.2	14.5	7.9
8	Thermal-bonded GCLs W-NW	25	28.9	38.7	19.1	25	12.9	18.1	7.7
9	Needle-punched NW-NW	17	37.1	58.4	15.8	5	10.8	14.3	7.2
10	Thermal-bonded GCLs NW-NW	21	26.8	42.0	11.6	18	9.9	13.7	6.0
11	GCL A	219	30.6	47.9	13.4	152	11.2	14.4	8.0

Note: Only tests with σ_n below 550 kPa were used to define ϕ_{EQ} values. Not all tests reported for τ_p reach τ_{ld} .

Table 3: Failure Envelopes for GCL F

Series Name	Normal Stress (kPa)	Peak Shear Strength (kPa)	Large Displacement Shear Strength (kPa)	τ_{LD}/τ_p	t_H (hrs)	Hydration Normal Stress (kPa)	t_C (hrs)	Consolidation Normal Stress (kPa)	Shear Displacement Rate (mm/min)	Final Water Content (%)
1	13.8	4.8	4.1	0.9	168	13.8	0	0.0	1.0	252.5
	27.6	7.6	6.2	0.8	168	27.6	0	0.0	1.0	252.5
	55.2	13.8	10.3	0.8	168	55.2	0	0.0	1.0	252.5
2a	275.8	38.6	35.2	0.9	0	0.0	14	275.8	0.1	34.0
2b	68.9	20.7	14.5	0.7	0	0.0	0	0.0	1.0	84.0
	275.8	33.8	30.3	0.9	0	0.0	0	0.0	1.0	84.0
	482.6	47.6	43.4	0.9	0	0.0	0	0.0	1.0	84.0
3	9.6	3.3	2.3	0.70	24	9.58	0	0	1	#N/A
	9.6	3.4	2.7	0.80	24	9.58	0	0	1	#N/A
	9.6	3.7	3.3	0.88	24	9.58	0	0	1	#N/A
	9.6	4.6	3.3	0.71	24	9.58	0	0	1	#N/A
	9.6	3.4	3.0	0.88	24	9.58	0	0	1	#N/A
	9.6	5.1	3.5	0.70	24	9.58	0	0	1	#N/A

Table 4: Shear Strength Variability Analysis for Different GCLs

Analysis number	GCL name	Test conditions				Number of tests	Peak			Large-displacement		
		t_H (hs)	t_C (hs)	SDR (mm/min)	σ_n (kPa)		$E(\tau_p)$ (kPa)	$s(\tau_p)$ (kPa)	COV	$E(\tau_{id})$ (kPa)	$s(\tau_{id})$ (kPa)	COV
1	A	168	48	0.1	34.5	34	38.8	10.3	0.26	20.4	6.90	0.34
2	A	168	48	0.1	137.9	34	94.5	22.0	0.23	37.5	8.45	0.23
3	A	168	48	0.1	310.3	34	176.3	33.6	0.19	63.1	11.78	0.19
4	A	48	0	1.0	9.6	19	30.5	6.1	0.20	#N/A	#N/A	#N/A
5	F	24	0	1.0	9.6	6	3.9	0.7	0.19	3.0	0.5	0.15
6	A	24	0	1.0	9.6	5	25.1	1.1	0.05	#N/A	#N/A	#N/A
7	B	48	0	1.0	9.6	5	26.4	3.3	0.12	#N/A	#N/A	#N/A
8	A	0	0	1.0	517.1	5	404.4	41.4	0.10	232.1	26.83	0.12

Table 5: Failure Envelopes for the Interface between GCL K and a THDPE Geomembrane

Series Name	GCL Name	Geomembrane Name	Normal Stress (kPa)	Peak Shear Strength (kPa)	Large Displacement Shear Strength (kPa)	Hydration Time (hrs)	Hydration Normal Stress (kPa)	Final GCL Water Content (%)
1	K	60-mil s	68.9	58.6	54.5	0	0	15.3
	K	60-mil s	206.8	115.8	111.0	0	0	15.1
	K	60-mil s	344.7	187.5	111.0	0	0	15
2	K	60-mil s	96.5	36.5	19.3	24	96.5	#N/A
	K	60-mil s	193.1	64.1	42.1	24	193.1	#N/A
	K	60-mil s	386.1	134.4	82.7	24	386.1	#N/A
	K	60-mil s	482.6	157.2	97.9	24	482.6	#N/A
3	K	60-mil u	241.3	120.0	71.7	48	241.3	131.6
	K	60-mil u	482.6	245.5	148.2	48	482.6	131.6
	K	60-mil u	723.9	386.1	242.0	48	723.9	131.6
	K	60-mil u	965.3	483.3	288.2	48	965.3	131.6

Table 6: Shear Strength of the Interface between GCL A and an 80-mil Textured HDPE Geomembrane s ($t_H = 168$ hours, $t_C = 48$ hours, SDR = 0.1 mm/min)

Series Number	Shear Strength Data						Peak Failure Envelope		Large Displacement Failure	
	Normal Stress (kPa)	Peak Shear Strength (kPa)	Large Displacement Shear Strength (kPa)	τ_p/σ	τ_{LD}/σ	τ_{LD}/τ_p	Peak Friction Angle (Degrees)	Peak Intercept (kPa)	Large Displacement Friction Angle (Degrees)	Large Displacement Intercept (kPa)
1	34.5	20.0	13.8	0.58	0.40	0.69	20.70	4.92	13.47	2.36
	137.9	53.8	30.3	0.39	0.22	0.56				
	310.3	123.4	78.6	0.40	0.25	0.64				
2	34.5	17.2	13.8	0.50	0.40	0.80	20.99	1.48	12.37	4.92
	137.9	50.3	33.1	0.37	0.24	0.66				
	310.3	127.0	73.8	0.39	0.24	0.60				
3	34.5	20.0	12.4	0.58	0.36	0.62	16.12	7.29	11.68	2.36
	137.9	42.7	26.2	0.31	0.19	0.61				
	310.3	98.6	68.3	0.32	0.22	0.69				
4	34.5	19.3	13.1	0.56	0.38	0.68	18.32	7.19	11.04	6.30
	137.9	51.7	33.1	0.38	0.24	0.64				
	310.3	110.3	66.9	0.36	0.22	0.61				
5	34.5	17.2	11.0	0.50	0.32	0.64	16.83	5.12	9.63	3.74
	137.9	44.1	24.8	0.32	0.18	0.56				
	310.3	100.0	57.7	0.32	0.18	0.57				
6	34.5	16.5	11.0	0.48	0.32	0.67	20.45	6.89	12.24	7.39
	137.9	63.4	43.4	0.46	0.32	0.68				
	310.3	120.7	72.4	0.39	0.23	0.60				
7	34.5	19.3	9.7	0.56	0.28	0.50	26.03	5.32	14.27	1.38
	137.9	77.2	37.2	0.56	0.27	0.48				
	310.3	155.1	80.0	0.50	0.26	0.52				
8	34.5	18.6	12.4	0.54	0.36	0.67	15.83	15.07	12.61	5.61
	137.9	64.1	37.9	0.47	0.28	0.59				
	310.3	99.3	74.5	0.32	0.24	0.75				
9	34.5	14.5	9.7	0.42	0.28	0.67	16.50	12.12	12.01	3.94
	137.9	65.5	35.9	0.48	0.26	0.55				
	310.3	99.3	68.9	0.32	0.22	0.69				
10	34.5	21.1	13.1	0.70	0.38	0.54	21.77	5.61	9.78	7.19
	137.9	53.1	31.0	0.39	0.23	0.58				
	310.3	132.4	60.7	0.43	0.20	0.46				
11	34.5	18.6	11.7	0.54	0.34	0.63	20.09	2.07	10.07	3.84
	137.9	46.2	25.5	0.34	0.18	0.55				
	310.3	117.9	60.0	0.38	0.19	0.51				
12	34.5	18.6	14.5	0.54	0.42	0.78	16.38	12.71	10.05	10.34
	137.9	60.0	37.9	0.44	0.28	0.63				
	310.3	101.4	64.1	0.33	0.21	0.63				
13	34.5	16.5	12.4	0.48	0.36	0.75	20.86	0.98	12.52	3.35
	137.9	49.6	31.7	0.36	0.23	0.64				
	310.3	120.7	73.1	0.39	0.24	0.61				
14	34.5	27.6	15.2	0.80	0.44	0.55	27.20	10.64	14.28	5.02
	137.9	82.7	37.9	0.60	0.28	0.46				
	310.3	169.6	84.8	0.55	0.27	0.50				
15	34.5	25.5	15.9	0.74	0.46	0.62	23.85	12.31	15.86	6.70
	137.9	76.5	46.9	0.58	0.34	0.61				
	310.3	148.2	94.5	0.48	0.30	0.64				
16	34.5	31.7	19.3	0.92	0.56	0.61	22.89	20.78	14.69	10.44
	137.9	84.8	46.9	0.62	0.34	0.55				
	310.3	149.6	91.7	0.48	0.30	0.61				
17	34.5	21.4	13.8	0.62	0.40	0.65	23.24	3.55	13.05	4.53
	137.9	57.9	34.5	0.42	0.25	0.60				
	310.3	138.6	77.2	0.45	0.25	0.56				
18	34.5	17.2	14.5	0.50	0.42	0.84	23.04	5.81	13.68	5.42
	137.9	69.6	37.9	0.51	0.28	0.54				
	310.3	135.8	81.4	0.44	0.26	0.60				
19	34.5	18.6	11.7	0.54	0.34	0.63	20.23	6.89	13.10	1.87
	137.9	59.3	31.0	0.43	0.23	0.52				
	310.3	120.7	75.2	0.39	0.24	0.62				
20	34.5	19.3	13.8	0.56	0.40	0.71	20.76	1.77	10.34	5.81
	137.9	46.9	28.3	0.34	0.21	0.60				
	310.3	122.0	63.4	0.39	0.20	0.52				
21	34.47	15.44	8.48	0.45	0.25	0.55	24.56	1.40	14.23	2.46
	137.90	47.15	41.78	0.69	0.30	0.58				
	310.26	142.17	79.50	0.46	0.26	0.56				
22	34.47	15.31	7.93	0.44	0.23	0.52	20.42	4.69	14.02	2.06
	137.90	59.57	40.89	0.43	0.30	0.69				
	310.26	118.87	77.91	0.38	0.25	0.66				
23	34.47	15.72	8.00	0.46	0.23	0.51	20.38	4.97	12.72	2.93
	137.90	59.50	38.40	0.43	0.28	0.65				
	310.26	119.00	71.36	0.38	0.23	0.60				
24	34.47	18.13	9.95	0.53	0.29	0.55	26.89	1.37	14.16	4.98
	137.90	72.46	45.78	0.53	0.33	0.63				
	310.26	158.30	81.01	0.51	0.26	0.51				
25	34.47	13.24	8.69	0.38	0.25	0.66	20.62	4.95	11.97	4.54
	137.90	64.33	38.82	0.47	0.28	0.60				
	310.26	118.87	68.40	0.32	0.22	0.58				
26	34.47	20.96	15.53	0.61	0.45	0.74	18.28	15.24	10.75	10.68
	137.90	69.84	39.58	0.51	0.29	0.57				
	310.26	114.32	68.53	0.37	0.22	0.60				
27	34.47	15.93	13.51	0.46	0.39	0.85	18.86	6.47	12.51	7.33
	137.90	57.30	40.27	0.42	0.29	0.70				
	310.26	111.07	75.29	0.36	0.24	0.68				
28	34.47	16.55	14.82	0.48	0.43	0.90	19.60	7.48	10.06	11.73
	137.90	61.71	41.02	0.45	0.30	0.66				
	310.26	116.04	64.95	0.37	0.21	0.56				
29	34.47	18.06	13.86	0.52	0.40	0.77	21.40	4.29	10.22	9.20
	137.90	57.92	36.54	0.42	0.27	0.63				
	310.26	126.04	64.19	0.41	0.21	0.51				
30	34.47	15.03	11.58	0.40	0.34	0.77	20.98	4.22	12.62	4.74
	137.90	60.95	37.02	0.44	0.27	0.61				
	310.26	121.76	73.70	0.39	0.24	0.61				
31	34.47	16.55	11.93	0.48	0.35	0.72	22.01	3.42	13.18	5.12
	137.90	60.47	39.43	0.44	0.29	0.65				
	310.26	128.38	77.01	0.41	0.25	0.60				
32	34.47	18.00	14.69	0.52	0.43	0.82	22.78	4.58	11.96	10.28
	137.90	64.19	44.13	0.47	0.32	0.69				
	310.26	134.24	74.26	0.43	0.24	0.55				
33	34.47	20.06	14.75	0.58	0.45	0.74	19.01	11.46	12.95	9.14
	137.90	64.19	44.54	0.47	0.32	0.69				
	310.26	116.38	79.08	0.38	0.25	0.68				
34	34.47	14.89	10.14	0.43	0.29	0.68	17.79	4.49	10.04	7.59
	137.90	49.78	27.71	0.36	0.22	0.76				
	310.26	103.63	60.40	0.33	0.19	0.58				
35	34.47	14.00	12.13	0.41	0.35	0.87	19.98	4.31	14.38	6.18
	137.90	59.02	46.13	0.43	0.33	0.78				
	310.26	118.43	83.98	0.37	0.27	0.73				
36	34.47	13.93	11.24	0.40	0.33	0.81	20.21	4.41	12.35	5.93
	137.90	60.26	39.71	0.44	0.29	0.66				
	310.26	116.73	72.53	0.38	0.23	0.62				
37	34.47	14.34	12.41	0.42	0.36	0.87	20.75	4.51	12.51	8.32
	137.90	61.91	44.61	0.45	0.32	0.72				
	310.26	120.11	75.01	0.39	0.24	0.62				
38	34.47	13.72	10.27	0.40	0.30	0.75	20.51	4.69	11.03	8.89
	137.90	62.47	44.33	0.45	0.32	0.71				
	310.26	118.45	66.19	0.38	0.21	0.56				
39	34.47	15.65	9.72	0.45	0.28	0.63	18.04	4.82	11.38	4.07
	137.90	59.36	40.82	0.43	0.30	0.69				
	310.26	129.48	77.57	0.42	0.25	0.60				
41	34.47	18.48	13.79	0.54	0.40	0.75	19.61	10.19	15.03	4.91
	137.90	65.71	42.53	0.48	0.31	0.65				
	310.26	118.31	87.98	0.38	0.28	0.74				

Table 7: Internal Shear Strength of GCL A ($t_H = 168$ hours, $t_C = 48$ hours, SDR = 0.1 mm/min)

Series Name	Shear Strength Data						Peak Failure Envelope		Large Displacement Failure	
	Normal Stress (kPa)	Peak Shear Strength (kPa)	Displacement Shear Strength (kPa)	τ_p/σ	τ_{L1}/σ	τ_{L2}/τ_p	Peak Friction Angle (Degrees)	Peak Intercept (kPa)	Large Displacement Friction Angle (Degrees)	Large Displacement Intercept (kPa)
1	34.5	37.9	13.8	1.1	0.4	0.4	25.84	16.55	6.14	10.05
	137.9	75.8	24.8	0.6	0.2	0.3				
	310.3	169.6	43.4	0.5	0.1	0.3				
2	34.5	46.9	18.6	1.4	0.5	0.4	29.75	27.78	9.17	13.79
	137.9	107.6	37.2	0.8	0.3	0.3				
	310.3	204.8	63.4	0.7	0.2	0.3				
3	34.5	42.1	17.9	1.2	0.5	0.4	26.12	26.59	9.90	10.54
	137.9	96.5	32.4	0.7	0.2	0.3				
	310.3	177.9	65.5	0.6	0.2	0.4				
4	34.5	50.3	33.8	1.5	1.0	0.7	30.73	38.81	7.99	28.66
	137.9	135.1	47.6	1.0	0.3	0.4				
	310.3	217.9	72.4	0.7	0.2	0.3				
5	34.5	41.4	31.7	1.2	0.9	0.8	34.79	17.63	11.78	25.51
	137.9	113.8	55.8	0.8	0.4	0.5				
	310.3	233.0	89.6	0.8	0.3	0.4				
6	34.5	46.2	24.1	1.3	0.7	0.5	31.16	27.28	12.54	18.22
	137.9	113.8	51.7	0.8	0.4	0.5				
	310.3	213.7	86.2	0.7	0.3	0.4				
7	34.5	46.2	18.6	1.3	0.5	0.4	28.99	29.45	9.00	14.28
	137.9	109.6	37.9	0.8	0.3	0.3				
	310.3	199.9	62.7	0.6	0.2	0.3				
8	34.5	49.6	14.5	1.4	0.4	0.3	33.12	30.63	12.21	9.55
	137.9	126.2	43.4	0.9	0.3	0.3				
	310.3	231.0	75.2	0.7	0.2	0.3				
9	34.5	46.2	38.6	1.3	1.1	0.8	25.19	27.97	4.96	36.15
	137.9	89.6	49.0	0.7	0.4	0.5				
	310.3	175.1	62.7	0.6	0.2	0.4				
10	34.5	39.3	17.2	1.1	0.5	0.4	29.44	18.62	11.99	9.95
	137.9	94.5	39.3	0.7	0.3	0.4				
	310.3	194.4	75.8	0.6	0.2	0.4				
11	34.5	46.2	15.9	1.3	0.5	0.3	29.30	29.45	10.22	7.78
	137.9	111.0	29.6	0.8	0.2	0.3				
	310.3	202.0	64.8	0.7	0.2	0.3				
12	34.5	55.2	#N/A	1.6	#N/A	#N/A	33.73	37.13	#N/A	#N/A
	137.9	137.2	#N/A	1.0	#N/A	#N/A				
	310.3	241.3	#N/A	0.8	#N/A	#N/A				
13	34.5	49.0	8.3	1.4	0.2	0.2	21.26	36.25	6.62	1.77
	137.9	91.0	13.8	0.7	0.1	0.2				
	310.3	156.5	39.3	0.5	0.1	0.3				
14	34.5	44.1	15.2	1.3	0.4	0.3	21.64	39.60	5.40	13.99
	137.9	108.9	30.3	0.8	0.2	0.3				
	310.3	157.2	42.1	0.5	0.1	0.3				
15	34.5	53.1	31.0	1.5	0.9	0.6	28.01	45.41	7.84	26.10
	137.9	135.8	44.8	1.0	0.3	0.3				
	310.3	204.1	68.9	0.7	0.2	0.3				
16	34.5	43.4	11.7	1.3	0.3	0.3	32.84	22.56	9.95	5.32
	137.9	113.8	29.0	0.8	0.2	0.3				
	310.3	222.0	60.0	0.7	0.2	0.3				
17	34.5	58.6	32.4	1.7	0.9	0.6	26.24	44.82	6.84	28.27
	137.9	117.9	44.8	0.9	0.3	0.4				
	310.3	195.8	65.5	0.6	0.2	0.3				
18	34.5	51.7	9.7	1.5	0.3	0.2	25.42	36.84	7.51	7.29
	137.9	104.8	29.0	0.8	0.2	0.3				
	310.3	183.4	46.9	0.6	0.2	0.3				
19	34.5	44.1	21.4	1.3	0.6	0.5	31.88	24.72	11.21	14.09
	137.9	113.8	40.7	0.8	0.3	0.4				
	310.3	216.5	75.8	0.7	0.2	0.4				
20	34.47	30.34	19.99	0.88	0.58	0.66	23.05	15.29	8.51	15.31
	137.90	73.36	36.68	0.53	0.27	0.50				
	310.26	147.55	61.43	0.48	0.20	0.42				
21	34.47	30.34	19.99	0.88	0.58	0.66	23.03	15.21	9.18	15.77
	137.90	73.08	40.20	0.53	0.29	0.55				
	310.26	147.41	65.09	0.48	0.21	0.44				
22	34.47	22.20	15.24	0.64	0.44	0.69	21.59	8.35	8.13	11.04
	137.90	62.60	31.92	0.45	0.23	0.51				
	310.26	131.28	54.95	0.42	0.18	0.42				
23	34.47	27.37	15.24	0.79	0.44	0.56	24.74	11.17	8.57	10.25
	137.90	74.19	31.37	0.54	0.23	0.42				
	310.26	154.30	56.88	0.50	0.18	0.37				
24	34.47	28.13	22.27	0.82	0.65	0.79	23.05	15.68	7.48	18.75
	137.90	77.91	38.47	0.57	0.28	0.49				
	310.26	146.38	58.88	0.47	0.19	0.40				
25	34.47	27.37	19.24	0.79	0.56	0.70	23.11	12.69	8.16	13.84
	137.90	71.57	32.89	0.52	0.24	0.46				
	310.26	145.07	58.61	0.47	0.19	0.40				
26	34.47	30.47	18.82	0.88	0.55	0.62	25.77	13.45	7.64	13.61
	137.90	79.43	31.16	0.58	0.23	0.39				
	310.26	163.47	55.57	0.53	0.18	0.34				
27	34.47	32.34	17.93	0.94	0.52	0.55	25.17	17.98	8.79	13.40
	137.90	85.70	35.99	0.62	0.26	0.42				
	310.26	162.65	60.88	0.52	0.20	0.37				
28	34.47	30.82	16.41	0.89	0.48	0.53	23.07	17.01	8.29	12.80
	137.90	77.15	35.16	0.56	0.26	0.46				
	310.26	148.65	57.16	0.48	0.18	0.38				
29	34.47	32.82	21.10	0.95	0.61	0.64	16.90	24.47	6.30	17.73
	137.90	69.77	33.65	0.51	0.24	0.48				
	310.26	117.49	51.71	0.38	0.17	0.44				
30	34.47	29.85	20.96	0.87	0.61	0.70	26.39	12.29	7.40	16.91
	137.90	79.98	35.51	0.58	0.26	0.44				
	310.26	166.51	56.95	0.54	0.18	0.34				
31	34.47	27.58	25.86	0.80	0.75	0.94	21.21	16.50	6.56	22.38
	137.90	73.70	39.02	0.53	0.28	0.53				
	310.26	135.55	57.78	0.44	0.19	0.43				
32	34.47	28.61	23.10	0.83	0.67	0.81	23.27	13.36	10.72	18.08
	137.90	71.98	46.61	0.52	0.34	0.65				
	310.26	147.07	75.91	0.47	0.24	0.52				
33	34.47	24.61	22.20	0.71	0.64	0.90	22.10	13.69	11.44	15.85
	137.90	74.60	44.75	0.54	0.32	0.60				
	310.26	137.83	78.26	0.44	0.25	0.57				
34	34.47	25.10	20.13	0.73	0.58	0.80	23.70	10.45	10.67	15.42
	137.90	71.77	44.26	0.52	0.32	0.62				
	310.26	146.38	72.81	0.47	0.23	0.50				

Table 8: Statistical Analysis of the Shear Strength of the Interface between GCL A and an 80-mil Textured HDPE Geomembrane *s* Interface ($t_H = 168$ hours, $t_C = 48$ hours, SDR = 0.1 mm/min)

Statistical Values	Shear Strength Data						Failure Envelope			
	$\sigma = 34.5$ kPa		$\sigma = 137.9$ kPa		$\sigma = 310.3$ kPa		Peak		Large Displacement	
	Peak Shear Strength (kPa)	Large Displacement Shear Strength (kPa)	Peak Shear Strength (kPa)	Large Displacement Shear Strength (kPa)	Peak Shear Strength (kPa)	Large Displacement Shear Strength (kPa)	Friction Angle (Degrees)	Intercept Value (kPa)	Friction Angle (Degrees)	Intercept Value (kPa)
Average	18.03	12.33	60.77	37.81	122.86	73.44	20.66	6.40	12.40	5.79
St. Dev.	3.84	2.45	9.57	5.90	16.60	8.58	2.71	4.35	1.62	2.72
COV	0.21	0.20	0.16	0.16	0.14	0.12	0.13	0.68	0.13	0.47

Table 9: Statistical Analysis of the Internal Shear Strength of GCL A ($t_H = 168$ hours, $t_C = 48$ hours, SDR = 0.1 mm/min)

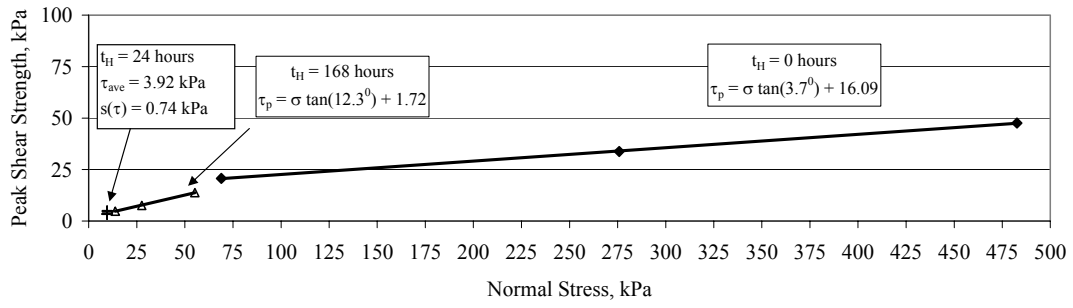
Statistical Values	Shear Strength Data						Failure Envelope			
	$\sigma = 34.5$ kPa		$\sigma = 137.9$ kPa		$\sigma = 310.3$ kPa		Peak		Large Displacement	
	Peak Shear Strength (kPa)	Large Displacement Shear Strength (kPa)	Peak Shear Strength (kPa)	Large Displacement Shear Strength (kPa)	Peak Shear Strength (kPa)	Large Displacement Shear Strength (kPa)	Friction Angle (Degrees)	Intercept Value (kPa)	Friction Angle (Degrees)	Intercept Value (kPa)
Average	38.81	20.39	94.51	37.54	176.29	63.13	26.22	23.40	8.76	15.53
St. Dev.	10.25	6.90	22.03	8.45	33.59	11.78	4.29	10.53	2.03	7.22
COV	0.26	0.34	0.23	0.23	0.19	0.19	0.16	0.45	0.23	0.46

Table 10: Summary of the Failure Envelope Data for the Shear Strength of the Interface between GCL A and an 80-mil Textured HDPE Geomembrane *s* and the Internal Shear Strength of GCL A ($t_H = 168$ hours, $t_C = 48$ hours, SDR = 0.1 mm/min)

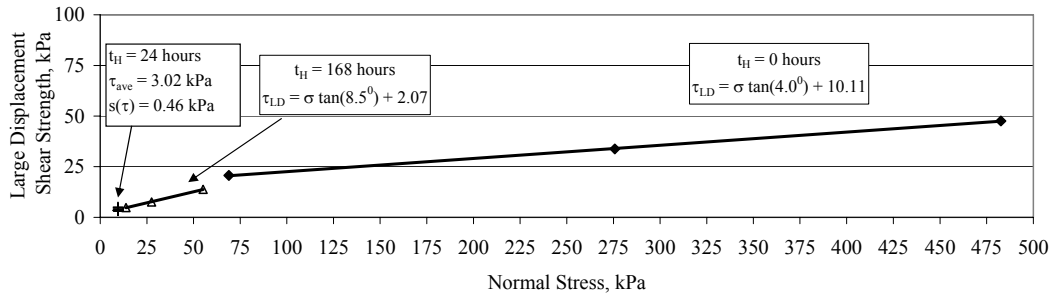
Statistical Values	Interface Failure Envelope				Internal Failure Envelope			
	Peak		Large Displacement		Peak		Large Displacement	
	Friction Angle (Degrees)	Intercept Value (kPa)	Friction Angle (Degrees)	Intercept Value (kPa)	Friction Angle (Degrees)	Intercept Value (kPa)	Friction Angle (Degrees)	Intercept Value (kPa)
Average	20.66	6.40	12.40	5.79	26.22	23.40	8.76	15.53
St. Dev.	2.71	4.35	1.62	2.72	4.29	10.53	2.03	7.22
COV	0.13	0.68	0.13	0.47	0.16	0.45	0.23	0.46
Correlation	-0.259		-0.344		0.316		-0.230	

Table 11: Peel Strength for GCL A; Included are the Series Number in Which the GCL was Tested for Internal or Interface Shear Strength in Tables 6 and 7

Sample Number	Internal Shear Strength Series Number	Interface Shear Strength Series Number	Specimen Number	Peel Strength (N)	Average Peel Strength (N)	Standard Deviation Peel Strength (N)	Sample Number	Internal Shear Strength Series Number	Interface Shear Strength Series Number	Specimen Number	Peel Strength (N)	Average Peel Strength (N)	Standard Deviation Peel Strength (N)
GCL 02-01	20	39/41	1	38.2	72.7	35.2	GCL 02-11	29	27	1	132.7	115.4	21.8
			2	122.1						2	144.4		
			3	41.8						3	95.3		
			4	69.5						4	105.1		
			5	91.8						5	99.4		
GCL 02-02	21	38	1	37.1	46.1	6.7	GCL 02-12	28	26	1	121.8	115.1	22.4
			2	44.9						2	149.9		
			3	44.3						3	106.2		
			4	55.3						4	90.4		
			5	49						5	107.1		
GCL 02-03	22	37	1	166.6	185.6	19.5	GCL 02-13	27	25	1	133.6	127.4	17.9
			2	198.5						2	141.1		
			3	164.7						3	144.7		
			4	189.3						4	102.7		
			5	208.8						5	115.1		
GCL 02-06	34	34/40	1	111.8	79.5	31.5	GCL 02-14	26	24	1	139.9	148.2	30.1
			2	34.4						2	199.7		
			3	83.1						3	144.5		
			4	104.5						4	121.2		
			5	63.8						5	135.9		
GCL 02-07	33	31/33	1	147	137.0	37.1	GCL 02-15	25	23	1	89.6	89.4	18.3
			2	75.8						2	62.2		
			3	132.2						3	89.8		
			4	159.6						4	113.7		
			5	170.5						5	91.7		
GCL 02-08	32	30	1	135	168.4	23.8	GCL 02-16	24	22	1	95.4	183.7	51.4
			2	158						2	186.6		
			3	167.9						3	224.4		
			4	195.6						4	198.6		
			5	185.7						5	213.4		
GCL 02-09	31	29	1	65.7	48.4	13.9	GCL 02-17	23	21/32	1	198	199.8	11.9
			2	56.1						2	198		
			3	31.3						3	184.4		
			4	51						4	217.6		
			5	37.7						5	201.1		
GCL 02-10	30	28	1	88.8	159.4	49.5				1	198		
			2	143.1						2	198		
			3	159.8						3	184.4		
			4	222.7						4	217.6		
			5	182.6						5	201.1		



(a)



(b)

Figure 1: Internal Shear Strength Failure Envelopes for GCL F (a) Peak, (b) Large Displacement

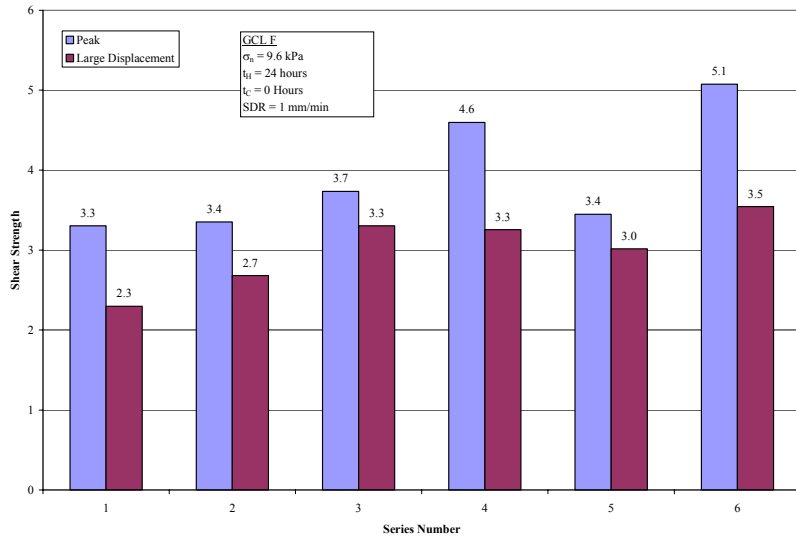
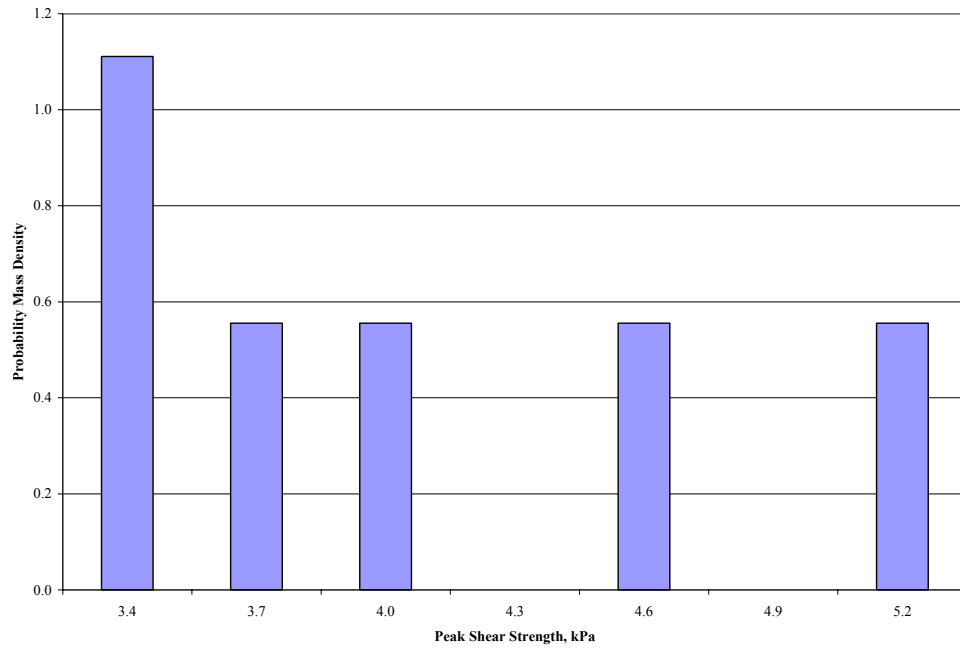
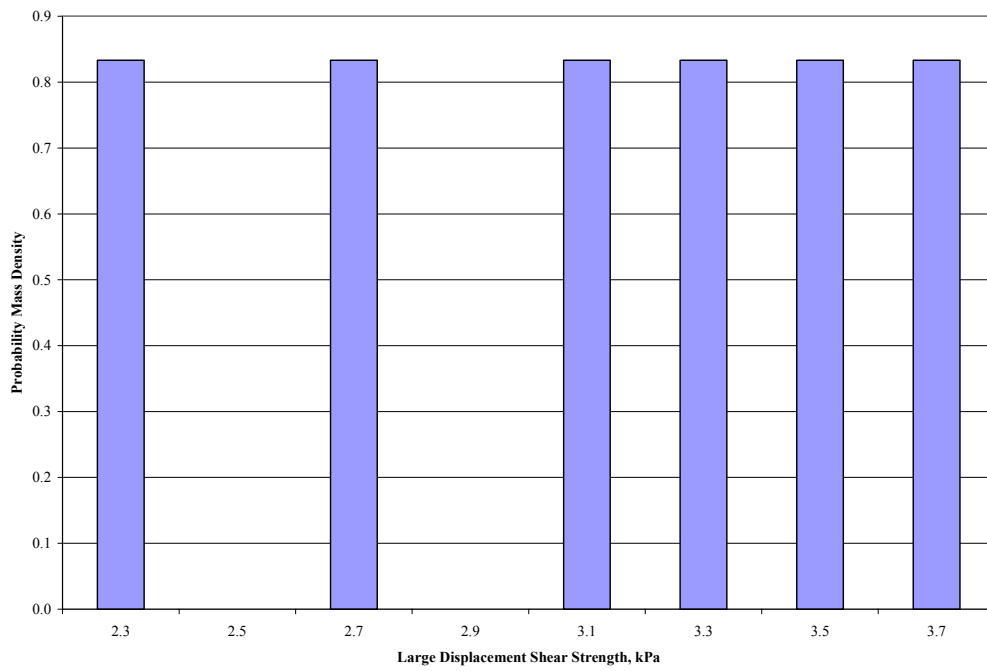


Figure 2: Variation in Peak and Large Displacement Shear Strength of GCL F Sheared at a Normal Stress of 9.6 kPa

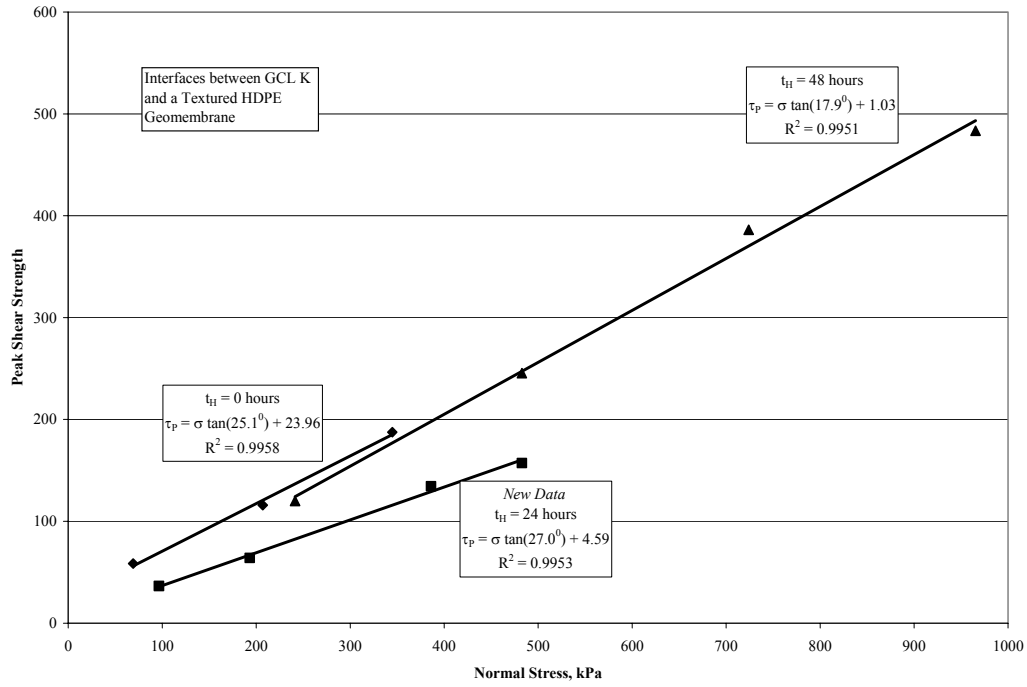


(a)

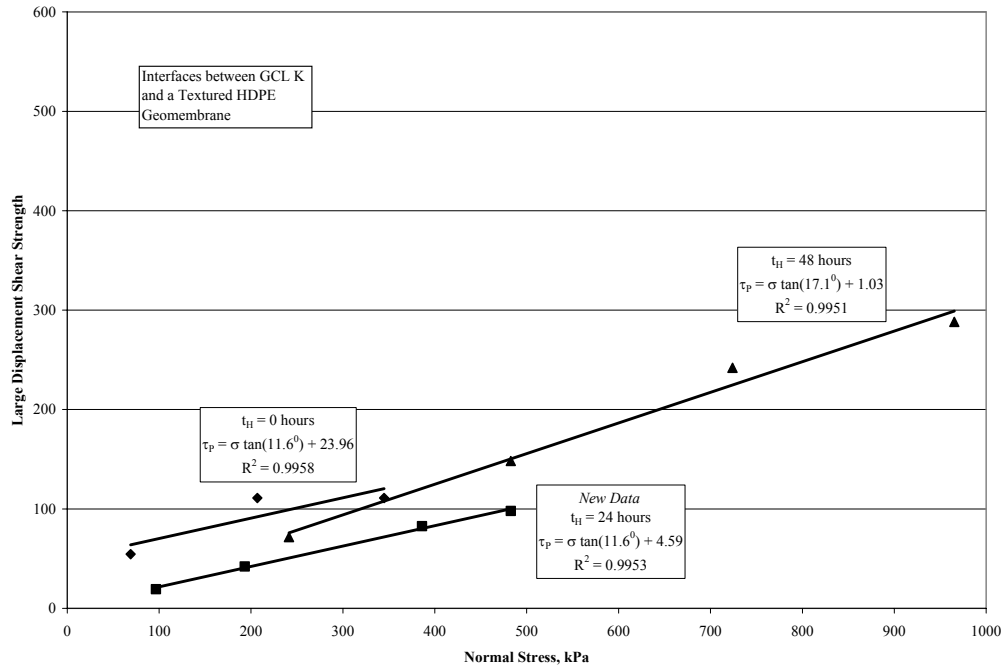


(b)

Figure 3: Probability Density Functions for the Shear Strength of GCL F: (a) Peak and (b) Large Displacement



(a)



(b)

Figure 4: Failure Envelopes for the Interface between GCL K and a Textured HDPE Geomembrane, Effect of the Time of Hydration (a) Peak, (b) Large Displacement

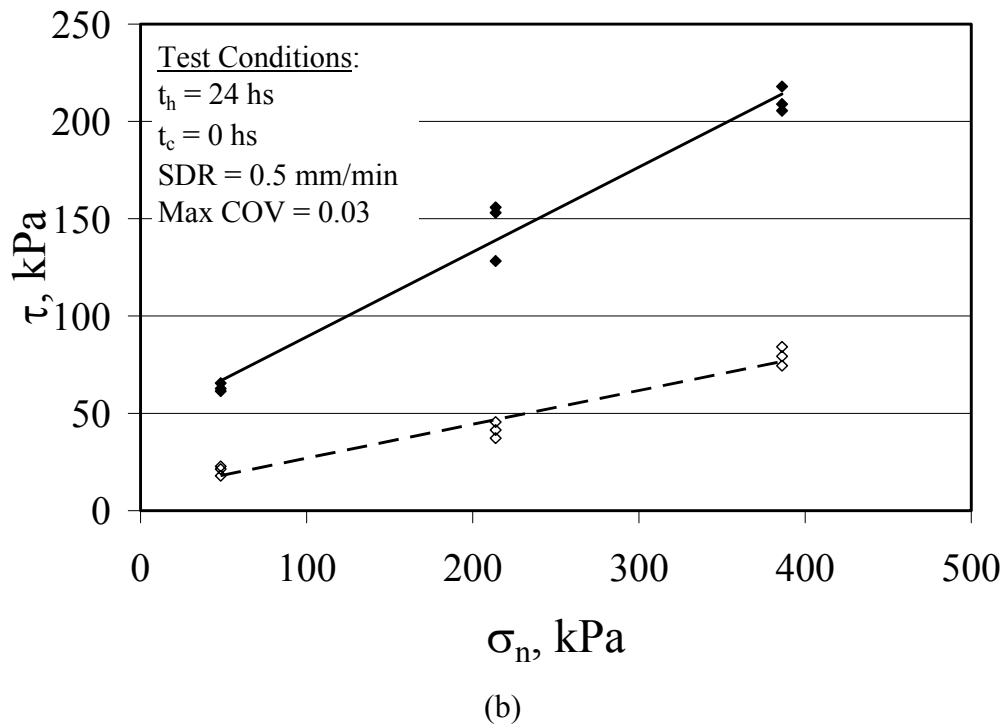
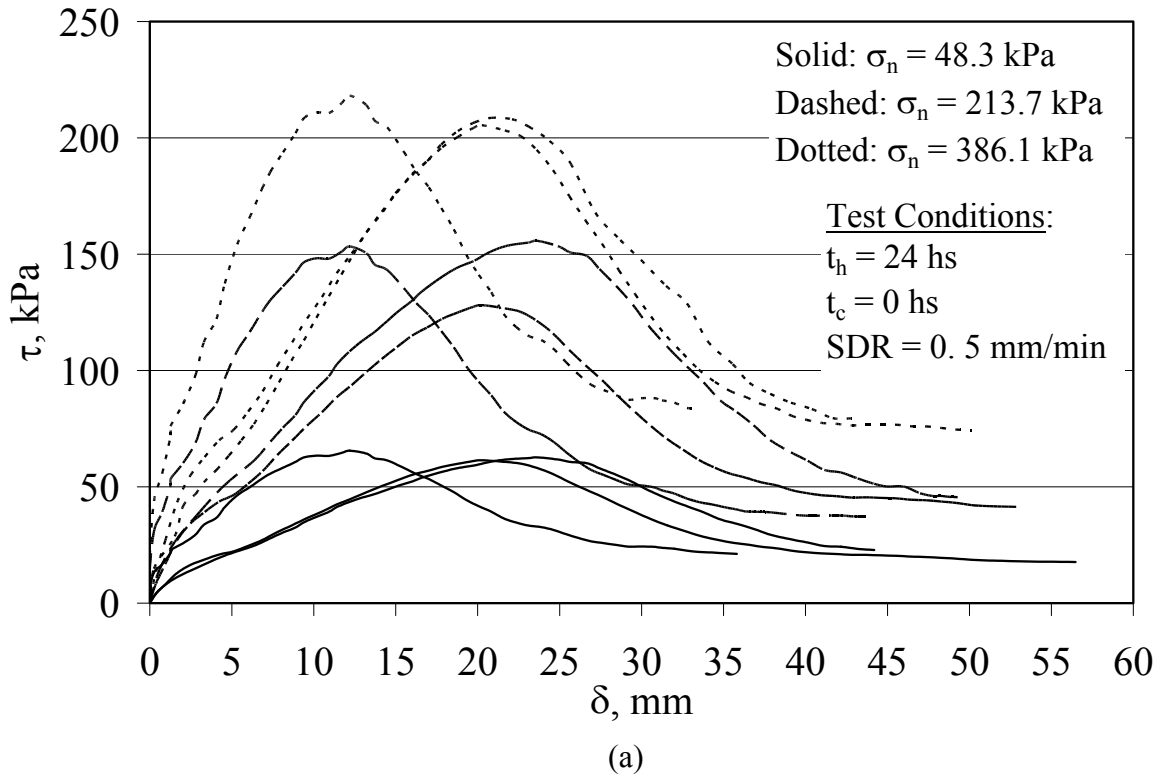
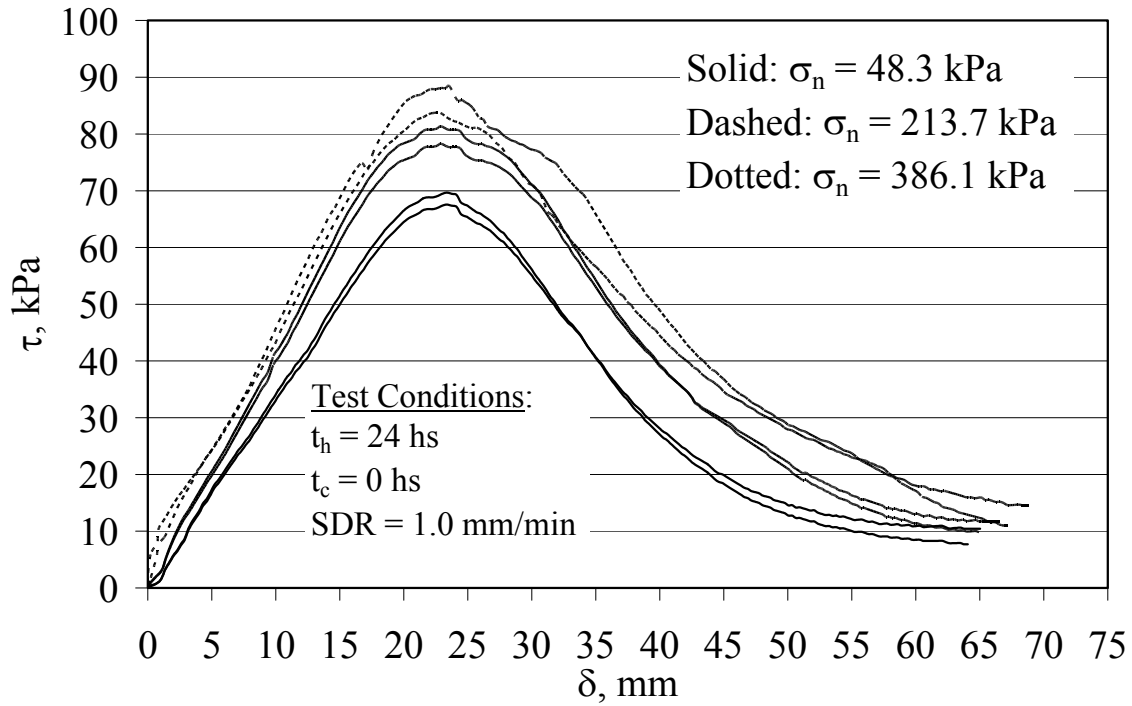
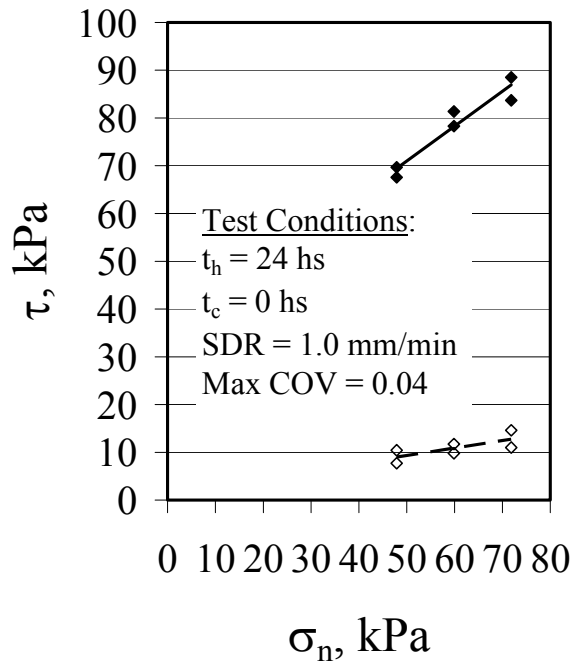


Figure 5: Repeatability of Shear Strength Tests on GCL A, $t_h = 24$ hs, $t_c = 0$ hs, SDR = 0.5 (Note: COV for each normal stress level is 0.01 to 0.03)

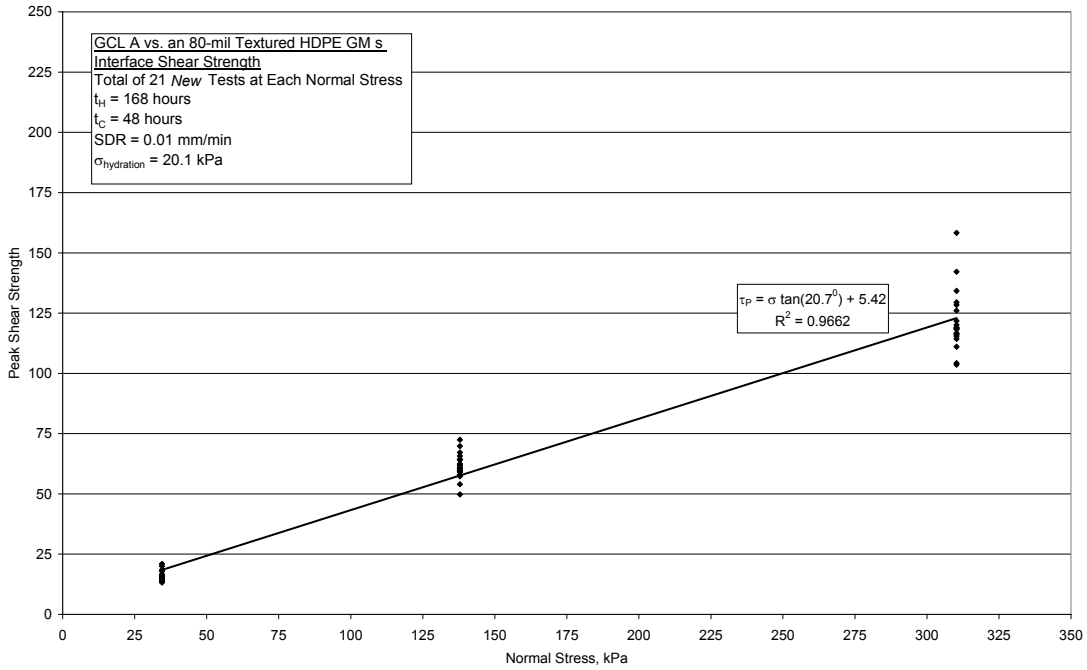


(a)

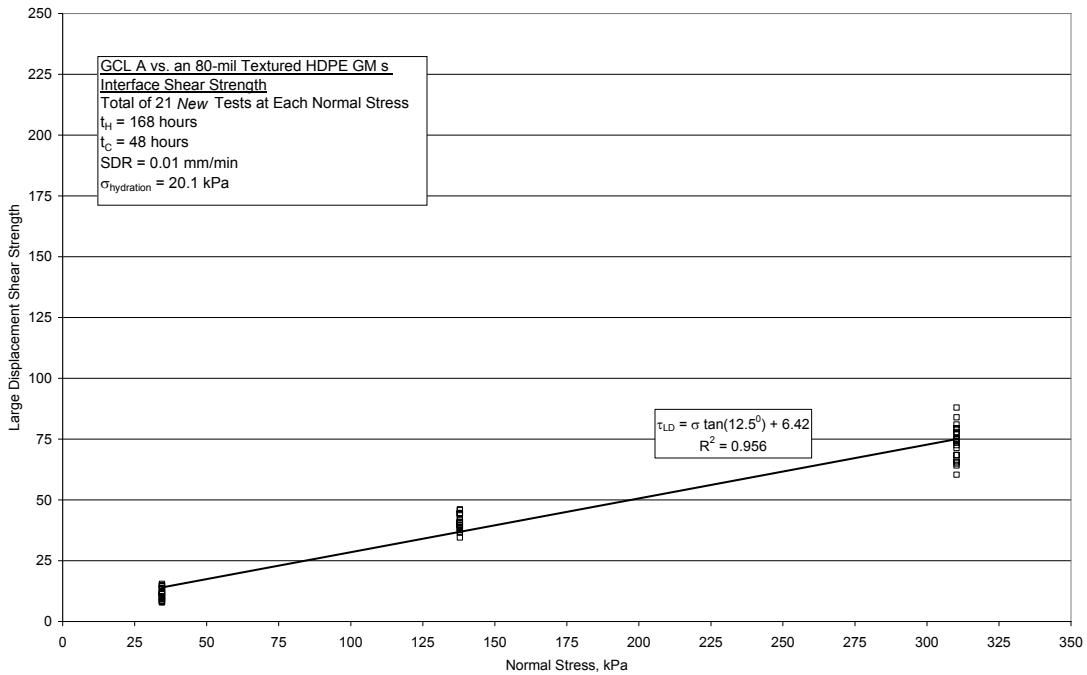


(b)

Figure 6: Repeatability of Shear Strength Tests on GCL A, $t_h = 24$ hs, $t_c = 0$ hs, SDR = 1.0 (Note: COV for each normal stress level is 0.02 to 0.05)

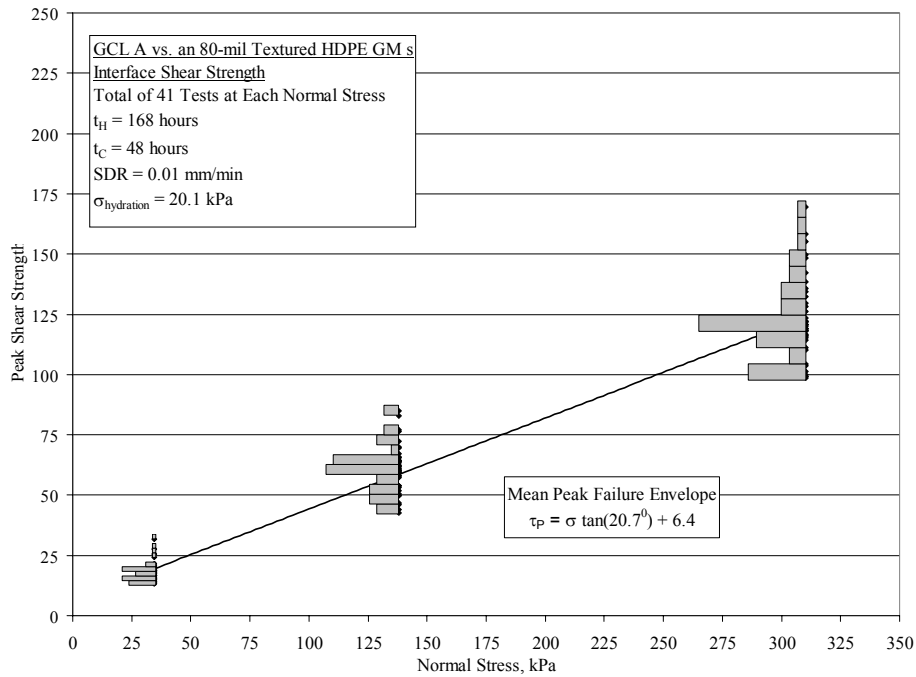


(a)

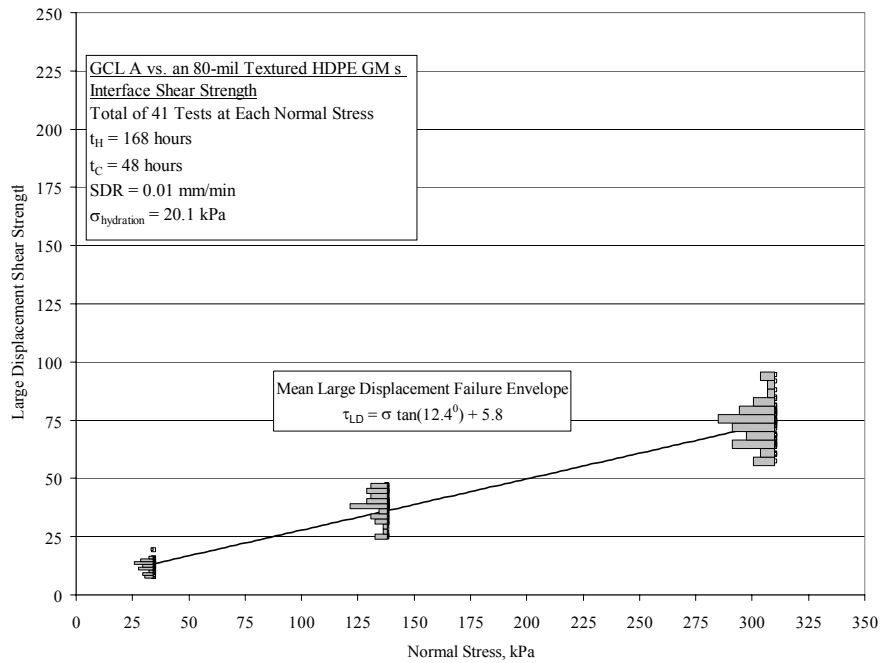


(b)

Figure 7: New Shear Strength Data for the Interface between GCL A and an 80-mil Textured HDPE Geomembrane s ($t_H = 168$ hours, $t_C = 48$ hours, SDR = 1.0 mm/min)

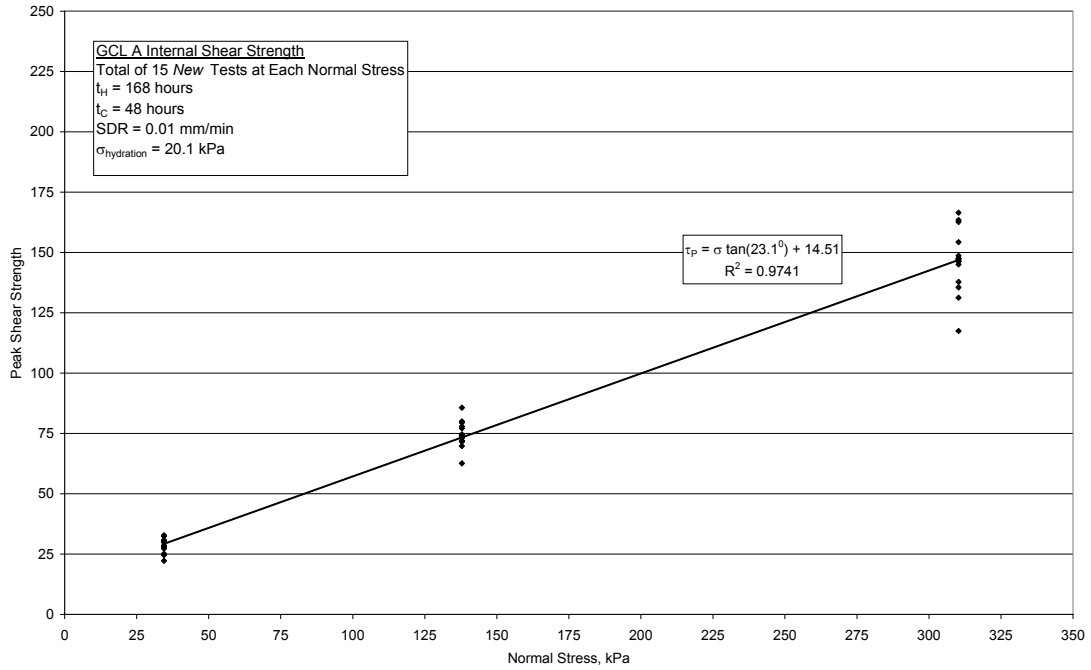


(a)

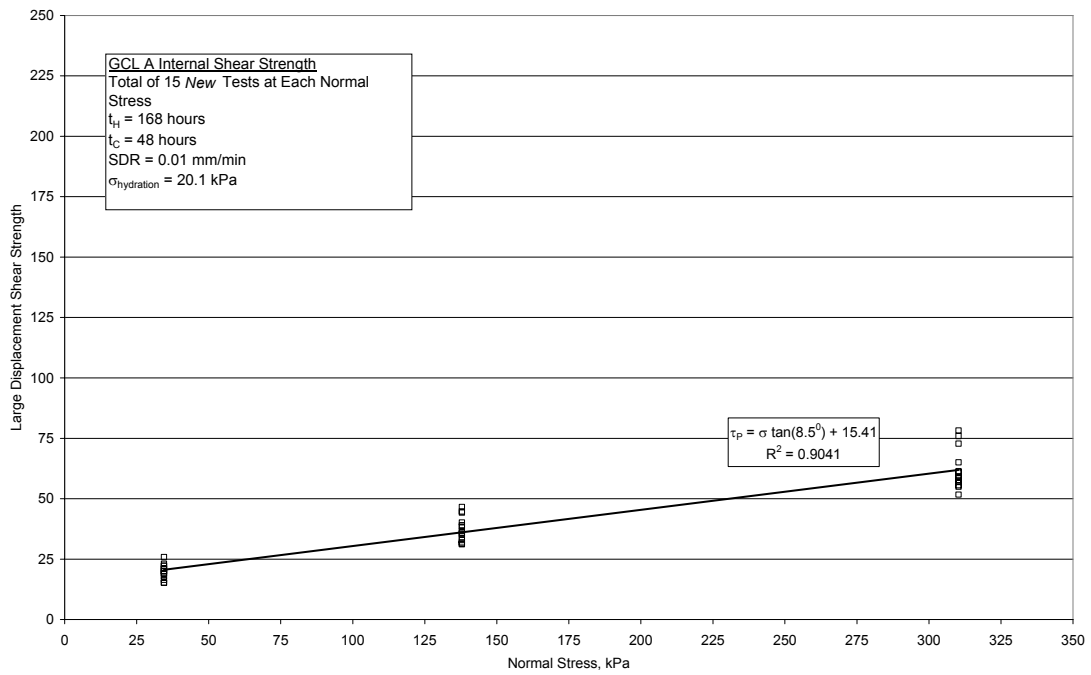


(b)

Figure 8: New Shear Strength Data Combined with Existing Data for the Interface between GCL A and an 80-mil Textured HDPE Geomembrane s ($t_H = 168$ hours, $t_C = 48$ hours, SDR = 1.0 mm/min)

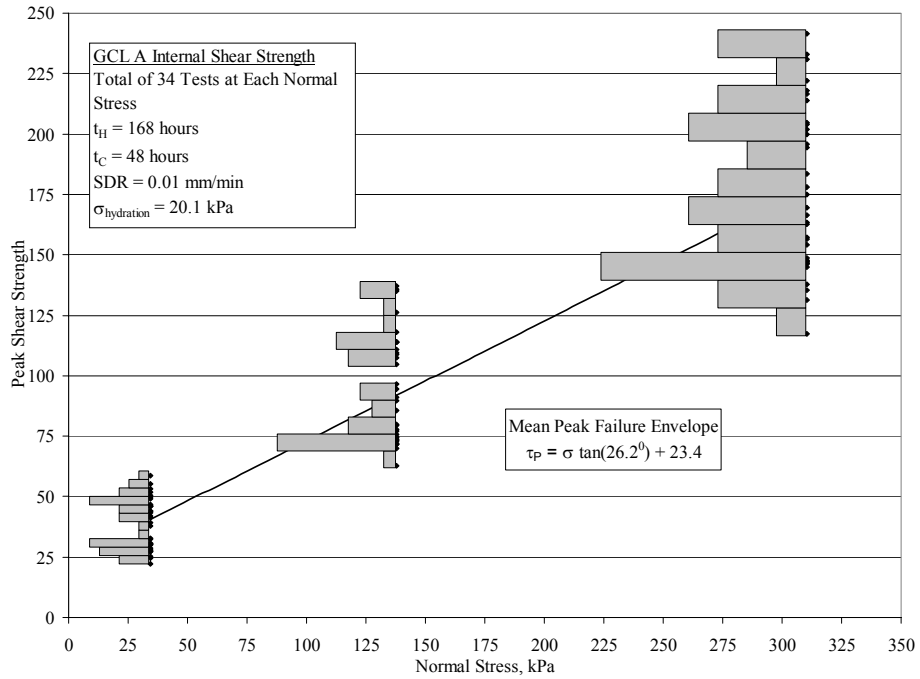


(a)

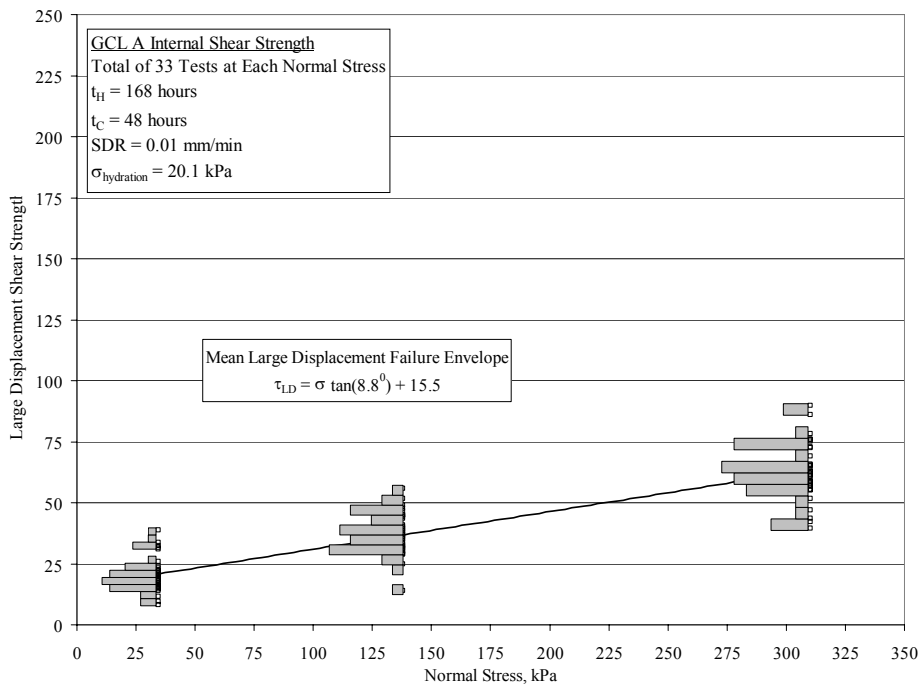


(b)

Figure 9: New Internal Shear Strength Data for GCL A ($t_H = 168$ hours, $t_C = 48$ hours, SDR = 1.0 mm/min)

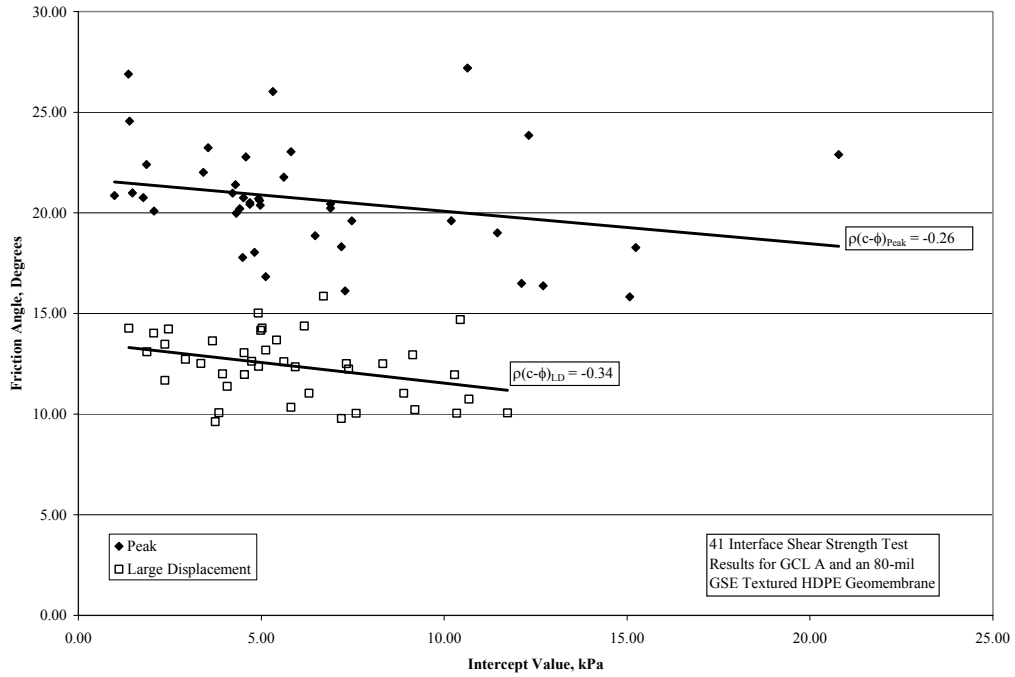


(a)

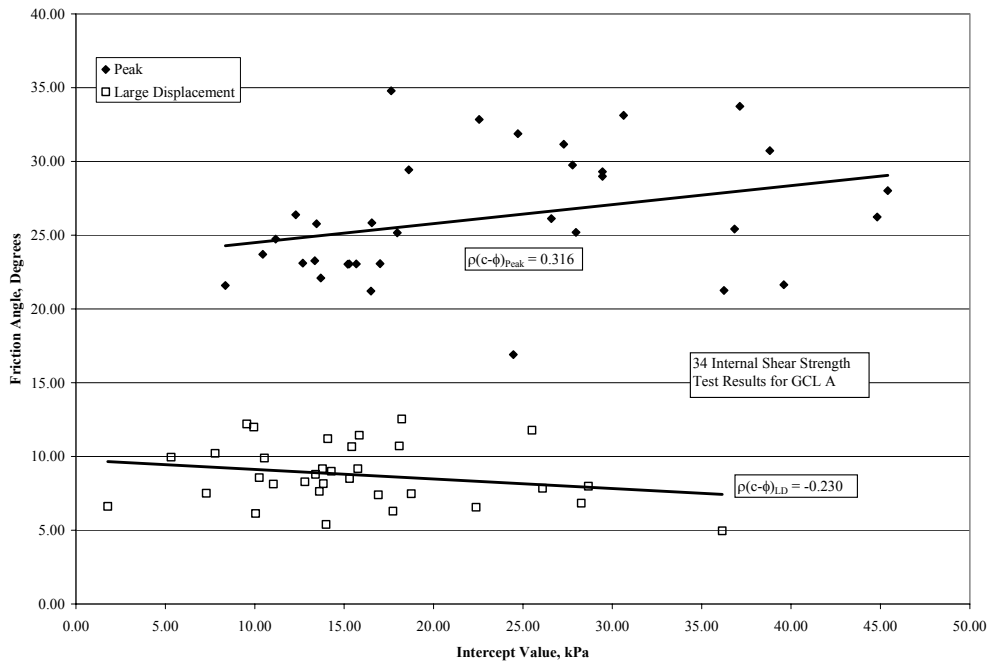


(b)

Figure 10: New Internal Shear Strength Data Combined with Existing Data for GCL A ($t_H = 168$ hours, $t_C = 48$ hours, SDR = 1.0 mm/min)

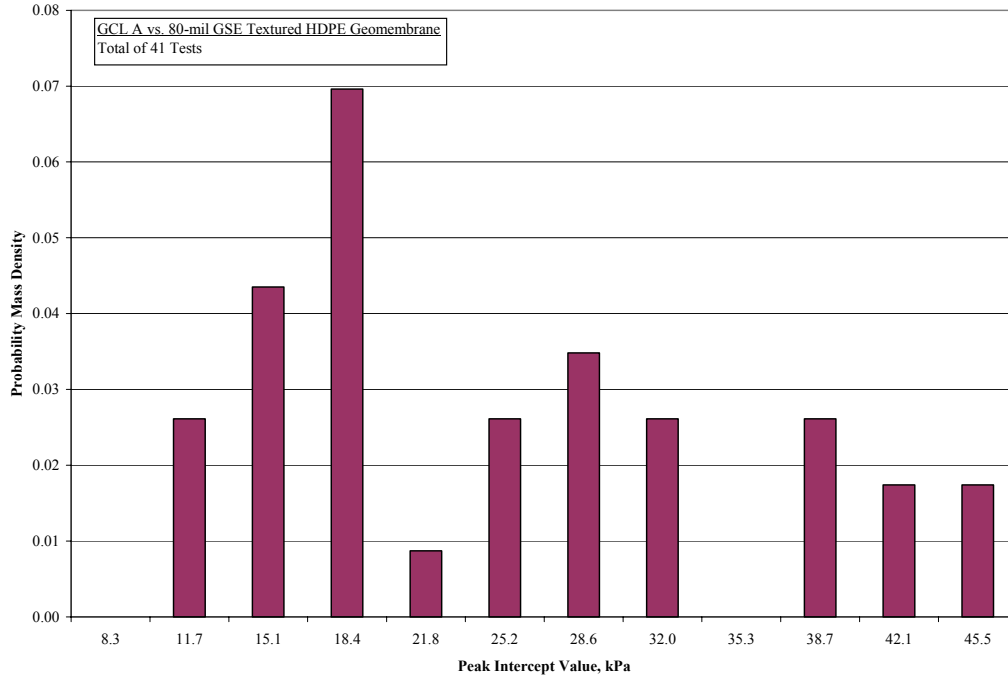


(a)

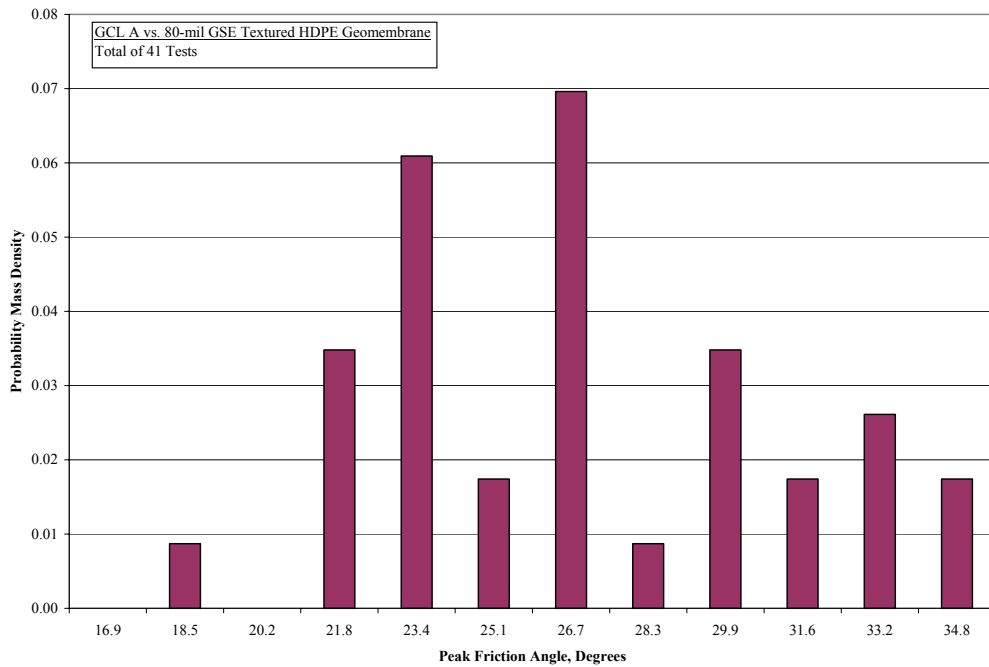


(b)

Figure 11: Correlation Plots for the Intercept Value and Friction Angle for the Peak and Large Displacement Shear Strength Failure Envelopes, (a) GCL A Interface with a Textured HDPE Geomembrane s, (b) Internal GCL A

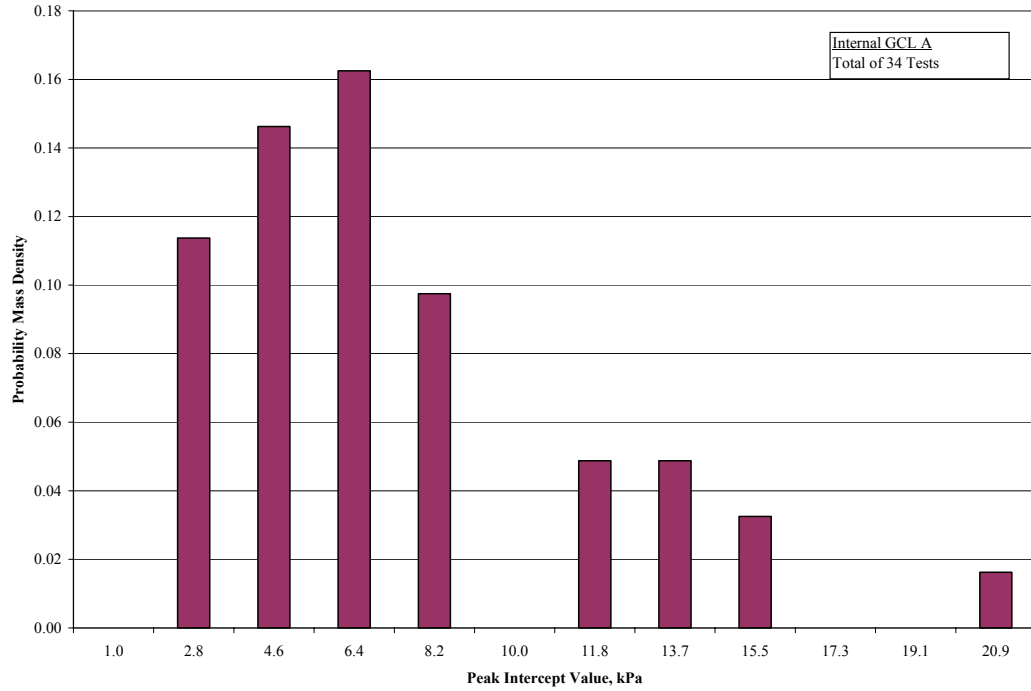


(a)

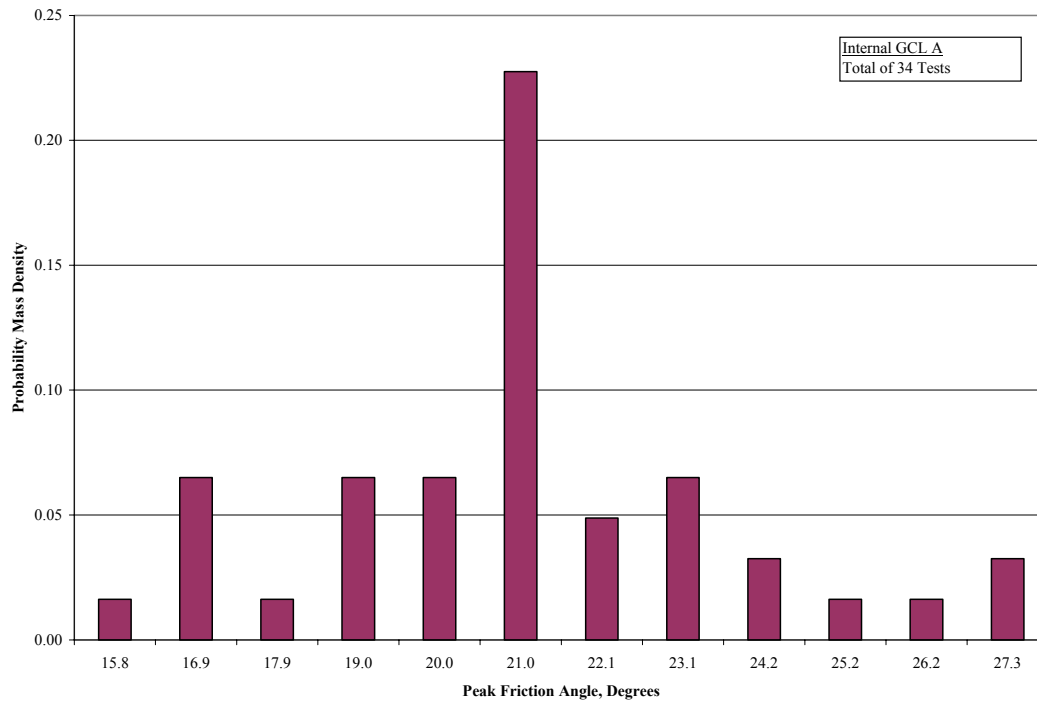


(b)

Figure 12: Probability Density Functions for the Peak Failure Envelope for the Interface between GCL A and a Textured HDPE Geomembrane s; (a) Intercept Value, (b) Friction Angle

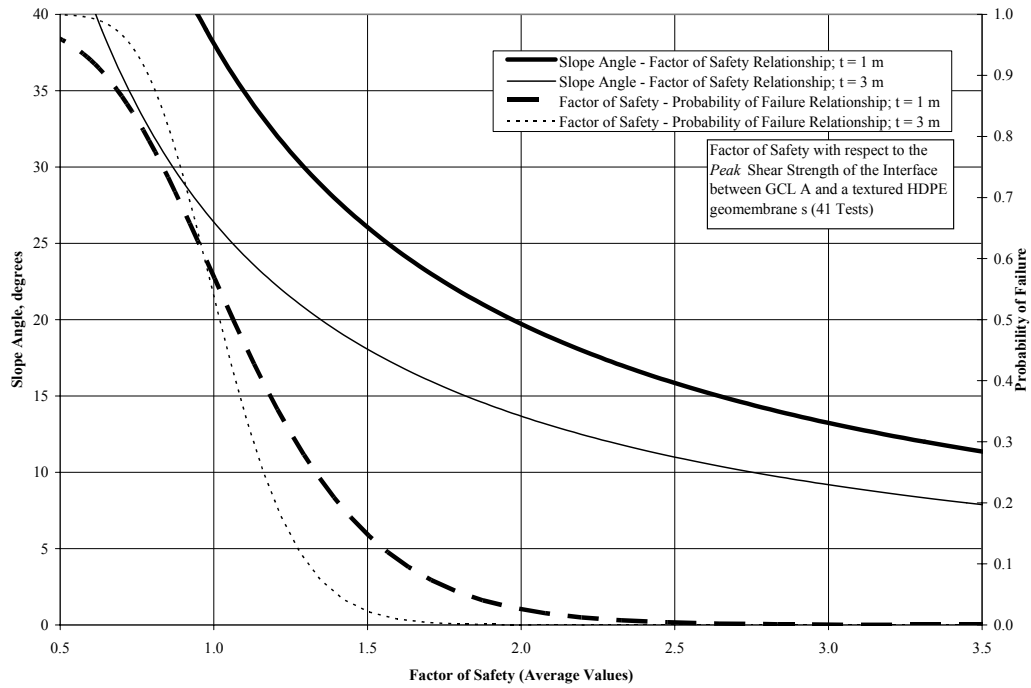


(a)

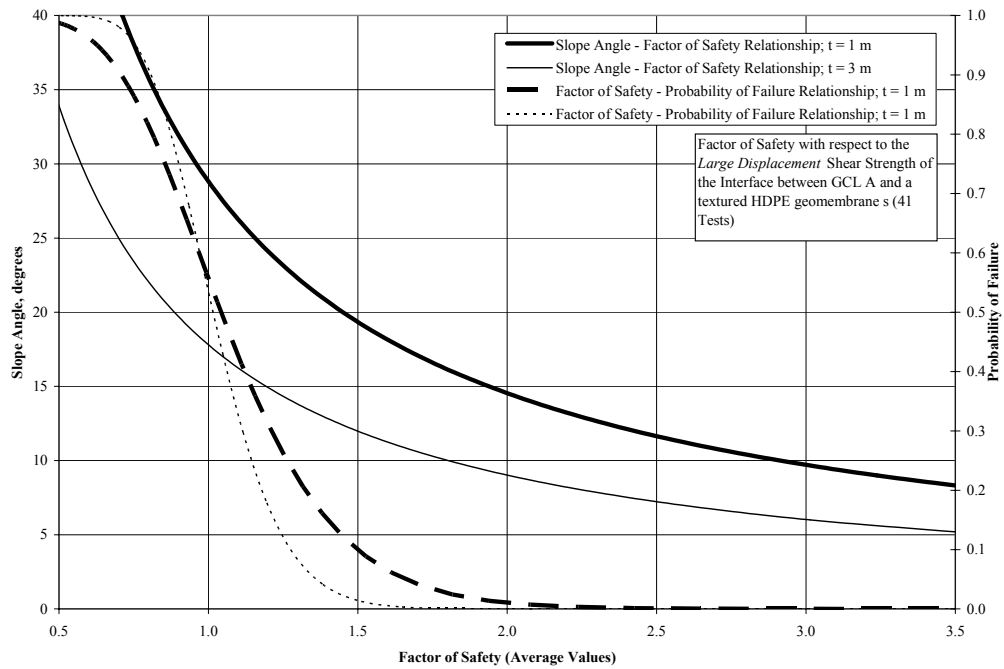


(b)

Figure 13: Probability Density Functions for the Peak Internal Failure Envelope for GCL A; (a) Intercept Value, (b) Friction Angle

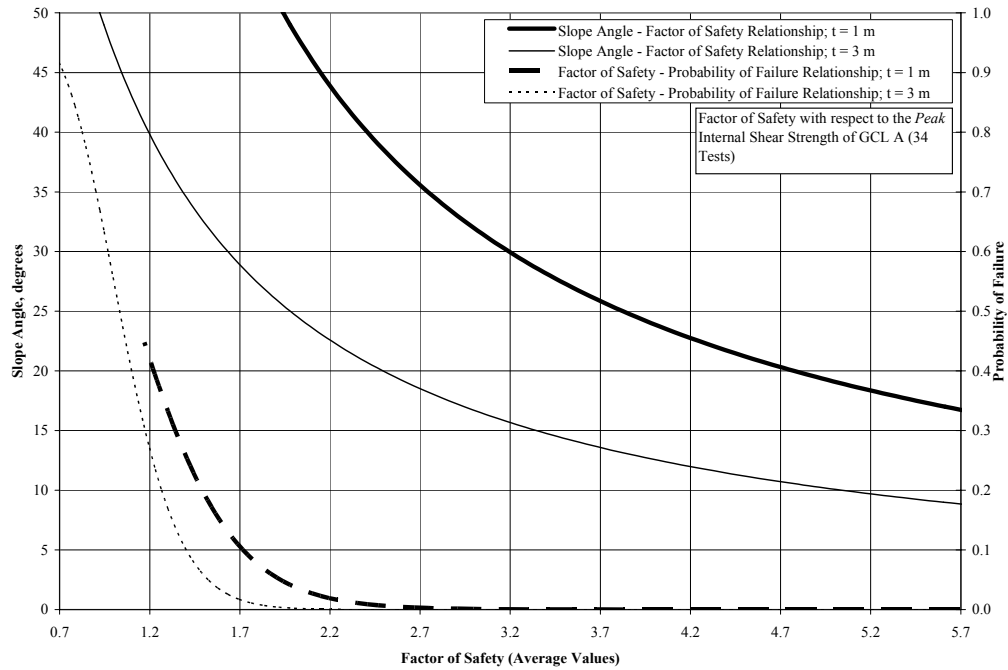


(a)

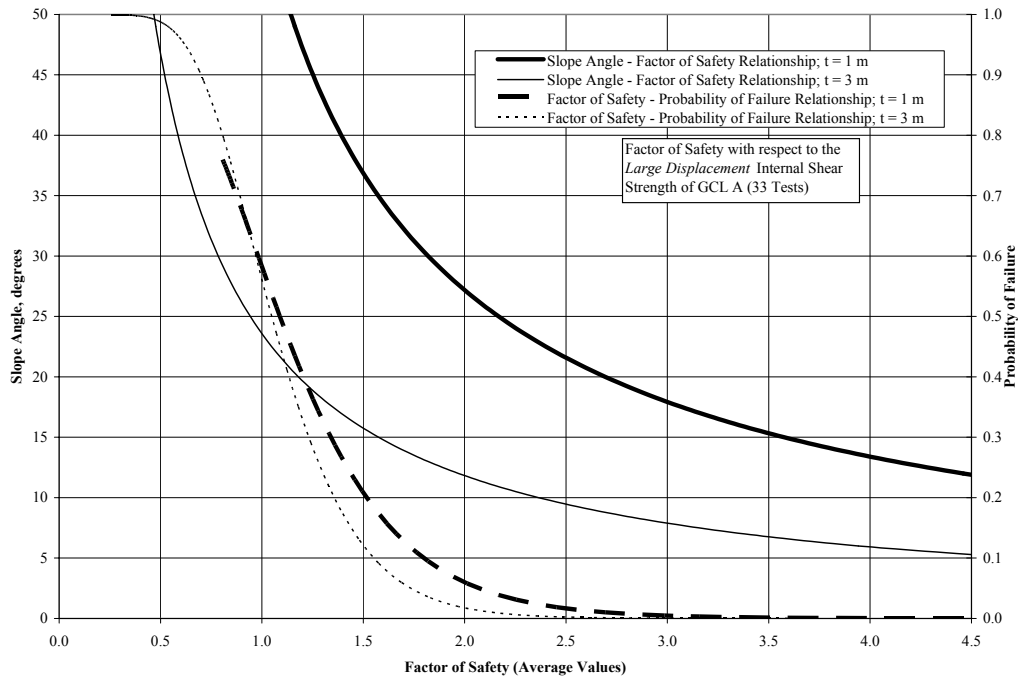


(b)

Figure 14: Modified Reliability Based Design Chart for for the Interface between GCL A and a Textured HDPE Geomembrane s; (a) Peak Shear Strength, (b) Large Displacement Shear Strength



(a)



(b)

Figure 15: Modified Reliability Based Design Chart for for the Interface between GCL A and a Textured HDPE Geomembrane s; (a) Peak Shear Strength, (b) Large Displacement Shear Strength

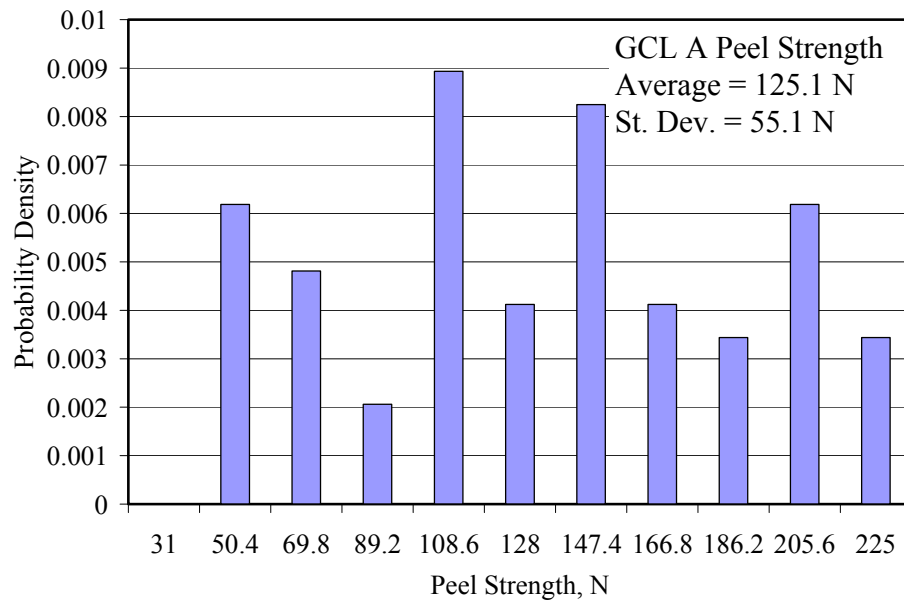


Figure 16: Probability Distribution for the Peel Strength of GCL A (5 Tests on 15 Specimens, Total of 75 Tests)

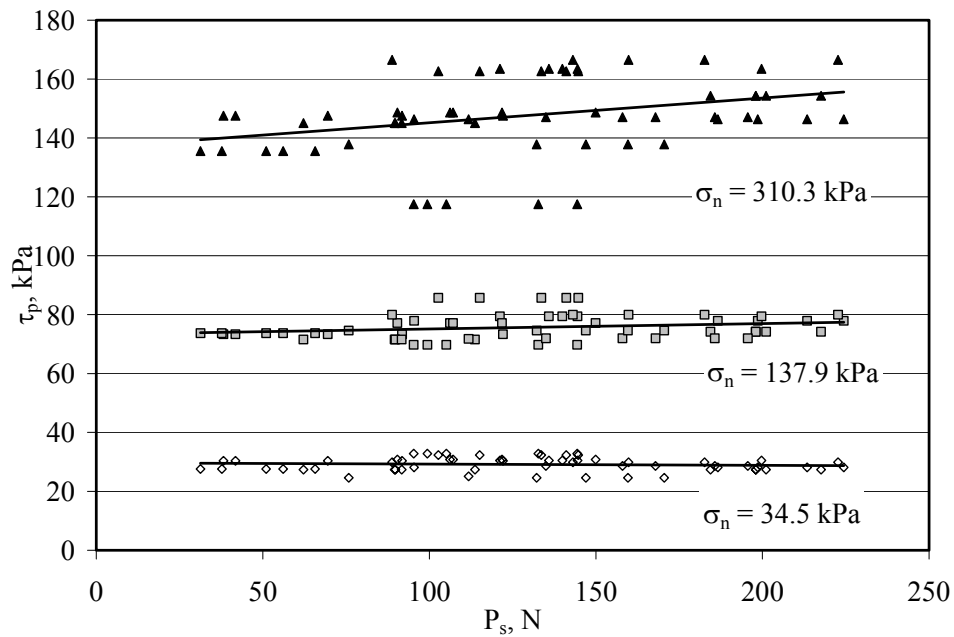
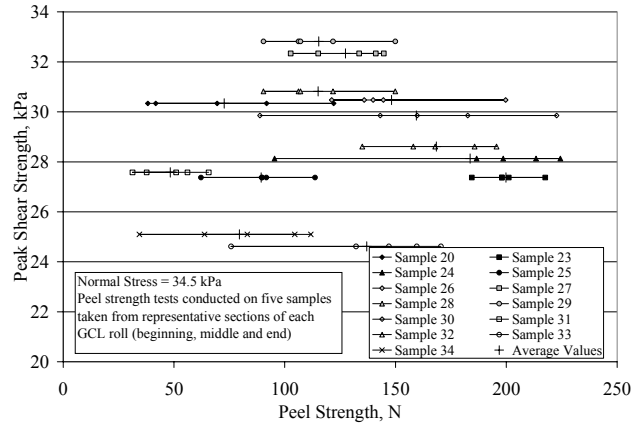
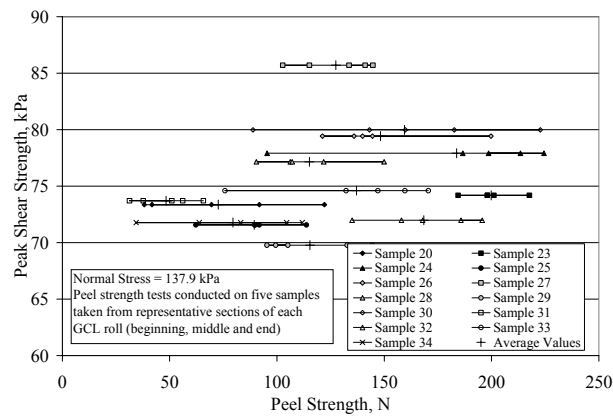


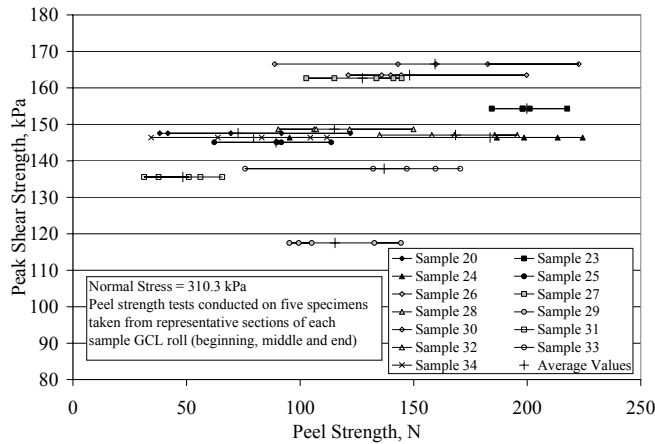
Figure 17: Relationship between Peel Strength and Peak Internal Shear Strength of GCL A



(a)



(b)



(c)

Figure 18: Relationships between Peel Strength and Peak Internal Shear Strength of GCL A for Normal Stresses of: (a) 34.5 kPa, (b) 137.9 kPa and (c) 310.3 kPa

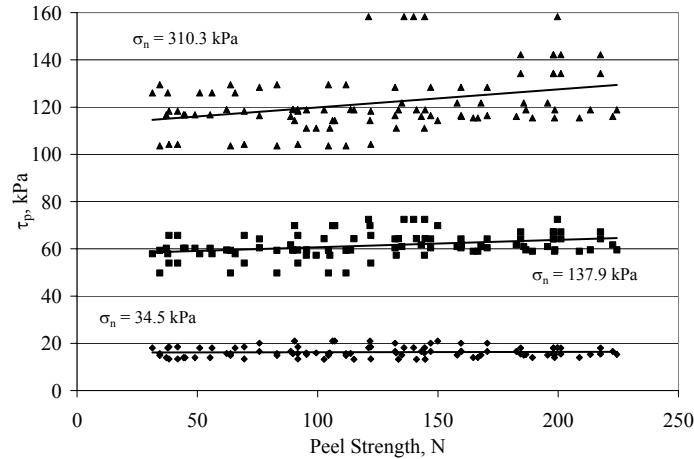
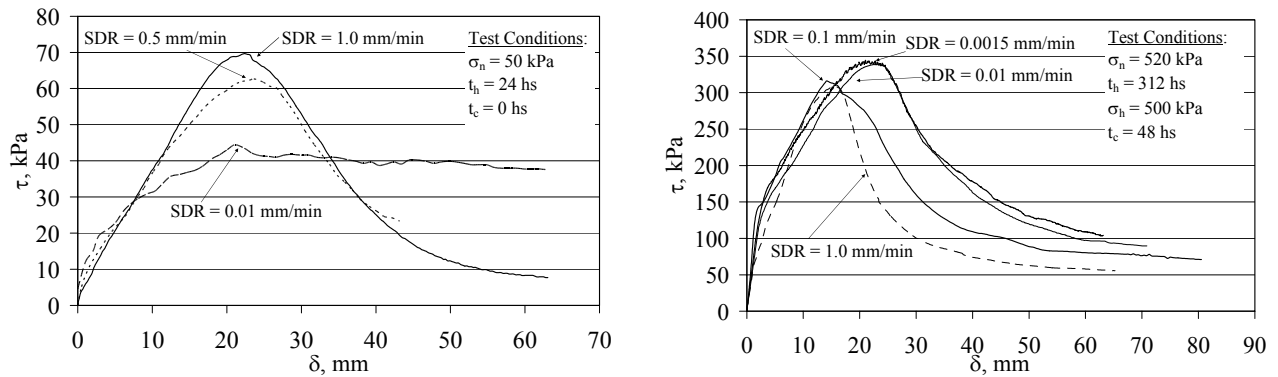
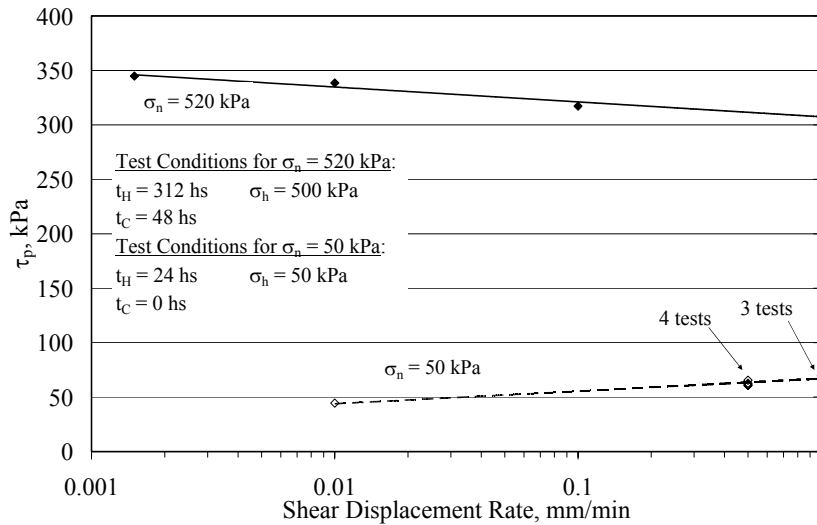


Figure 19: Relationship between Peel Strength and Peak Interface Shear Strength of GCL A



(a)



(c)

Figure 20: Effect of shear displacement rate on peak shear strength of GCL A for low σ_n (50 kPa) and high σ_n (520 kPa): (a) Shear stress-displacement curves for low σ_n , (b) Shear stress-displacement curves for high σ_n , (c) Summary trend of peak shear strength with SDR

Additional References

- Dixon, N., Kamugisha, P., and Jones, D. R. V. "Geosynthetic Interface Testing at Low Normal Stresses: Design and Implications." *7th International Conference on Geosynthetics*, Nice, Nice, France.
- Fox, P., Olsta, J., and Chiu, P. "Internal and Interface Shear Strengths of Needle-Punched Geosynthetic Clay Liners." *7th International Conference on Geosynthetics*, Nice, Nice, France.
- Jones, D. R. V., Dixon, N., and Connell, A. "Effect of Landfill Construction Activities on Mobilised Interface Shear Strength." *7th International Conference on Geosynthetics*, Nice, France.
- Blumel, W., Stoewahse, C., Dixon, N., Kamugisha, P., and Jones, D. R. V. "British-German Cooperative Research on Geosynthetic Friction Testing Methods." *7th International Conference on Geosynthetics*, Nice, Nice, France.
- Jones, D. R. V., and Dixon, N. "A Comparison of Geomembrane/Geotextile Interface Shear Strength by Direct Shear and Ring Shear." *7th International Conference on Geosynthetics*, Nice, Nice, France.
- McCartney, J. Zornberg, J. Swan, Jr. R. (2002). "Internal and Interface Shear Strength of Geosynthetic Clay Liners (GCLs)." *Report for the University of Colorado at Boulder, Department of Civil, Environmental and Architectural Engineering*.
- Zanziger, H. Alexiew, N. "New Shear Creep Tests on Stitch-Bonded GCLs: Important Results." *7th International Conference on Geosynthetics*, Nice, Nice, France.